ORIGINAL PAPER

Mahdieh Abbaslou · Ali Reza Saidi · Reza Bahaadini

Vibration and dynamic instability analyses of functionally graded porous doubly curved panels with piezoelectric layers in supersonic airflow

Abstract The present study, for the first time, investigates the vibration and flutter analyses of a doubly curved panel composed of functionally graded porous material contained by piezoelectric layers in supersonic flow. In this regard, the first-order piston theory for aerodynamic loading and Reddy's third-order shear deformation theory for doubly curved panel analysis is used. The governing equations of motion are obtained using Hamilton's principle and Maxwell's equation. The Galerkin method is used to discretize the equations of motion. Three types of piezoelectric layers are used, in both open-circuit and closed-circuit electrical boundary conditions. The FG porous material with three types of porosity structure is investigated, including uniform distribution, X-shaped distribution, and V-shaped distribution. Also, the effect of the power of the FG porous material and the porosity coefficient on the frequencies and the flutter boundaries of spherical, cylindrical, doubly curved shell with $R_y = -R_x$ and plate structures are investigated. The comparison of the spherical panel, doubly curved panel, cylindrical panel, and plate shows that the spherical panel has the highest and the plate has the lowest stability regions. Also, as the radius to length of the panel increases, the critical flutter aerodynamic pressure increases and the flutter frequency decreases. Furthermore, the effects of piezoelectricity, electrical and mechanical boundary conditions, geometric parameters, and the radii of curvatures on the flutter boundaries and flutter frequencies of FG porous doubly curved panels are investigated in detail.

1 Introduction

Aeroelastic instability can occur in both static and dynamic cases. One of the phenomena of dynamic instability discussed here is called flutter. Flutter is a type of dynamic instability of flying objects that results from the interaction of elastic, inertial, and aerodynamic forces. This phenomenon is a type of unstable vibrations of self-stimulation in which the structure receives its required energy from airflow and usually leads to accidental failure of the structure. The Flutter occurs when the aerodynamic forces of two vibration modes combine to give rise to this phenomenon. The vibration and instability characteristics of structures in supersonic flow have been analyzed in numerous studies. Krumhaar [1] studied the use of linear piston theory for cylindrical shells. The aeroelastic stability of the plates and shells was investigated by Dowell [2]. Pidaparti [3] performed the flutter analysis of the cantilevered curved composite panels. Cunningham et al. [4] studied the effects of various parameters such as ply orientation, geometric parameters, and boundary conditions on the dynamic behaviour of doubly curved composite panels. Kumar et al. [5] investigated the dynamic instability of the composite doubly curved panels. Zhang et al. [6] studied the flutter analysis of airfoils in supersonic flow using a local piston theory. Oh and Kim [7] investigated the dynamic instability of the cylindrical composite panels in supersonic flow. Hadadpour et al. [8] inspected the flutter characteristics for plates made of functionally graded material (FGM) in supersonic flow. Chorfi and Houmat [9] analyzed the nonlinear vibrations of the doubly curved shell.

M. Abbaslou · A. R. Saidi (✉) · R. Bahaadini
Department of Mechanical Engineering, Shahid Bahonar University of Kerman, Kerman, Iran
e-mail: saidi@uk.ac.ir

Hosseini and Fazelzadeh [10] investigated the aerothermoelastic and free vibration analysis of FGM panels. The vibration analysis of doubly curved panels was researched by Kiani et al. [11]. Aeroelastic characteristics of panels with different boundary conditions and neglecting and considering the shear deformation are investigated by Li and song [12]. Shen et al. [13] inspected the Nonlinear dynamic behaviour of a doubly curved panel. Wattanasakulpong and Chaikittiratana [14] investigated the vibration analysis of FGM doubly curved shell. Ganji and Dowell [15] predicted the flutter boundaries for two-dimensional flow. Graver et al. [16] studied the flutter behaviour of composite plates subjected to yawed supersonic flow. The flutter of composite doubly curved sandwich panels was investigated by Malekzadehfard et al. [17]. Sankar et al. [18] explored the flutter boundaries of doubly curved sandwich panels with carbon nanotube (CNT) reinforced face sheets.

Song et al. [19] researched the vibration characteristics of composite plates. Zare Jouneghani et al. [20] performed the vibration analysis of FG porous doubly curved panels. Rezaei et al. [21] investigated the vibration behaviour of plates composed of functionally graded porous materials. The vibration behaviour of doubly curved panels composed of functionally graded composite and carbon nanotube (CNT) was performed by Pouresmaeeli et al. [22]. Lie et al. [23] researched the dynamic stability of cylindrical panels reinforced with carbon nanotubes. Shahverdi et al. [24] investigated the aerothermoelastic analysis of functionally graded plates. Navazi and Haddadpour [25] performed the aeroelastic stability of panels composed of functionally graded materials. Kiani et al. [26] inspected the vibration analysis of composite conical panels reinforced with functionally graded carbon nanotubes. Mehar et al. [27] inspected the vibration characteristics of composite curved panels reinforced by carbon nanotubes. The aeroelastic analysis of curved composite panels was inspected by Zhou et al. [28]. Lin et al. [29] studied the nonlinear aeroelastic behaviour of the composite plate surrounded by a piezoelectric material layer. The aeroelastic behaviour of plates made of porous materials was inspected by Saidi et al. [30]. The flutter characteristics of thick porous plates were investigated by Bahaadini et al. [31]. Muc et al. [32] inspected the flutter of plate and shell structures. Arani et al. [33] studied the aeroelastic stability analysis of cylindrical panels reinforced with carbon nanotubes.

The flutter behavior of curved panels composed of porous material was investigated by Aditya et al. [34]. They studied the influences of parameters such as material properties, boundary conditions, and geometric properties on the stability of the system. Bahaadini et al. [35] inspected the dynamic stability of fluid-conveying thin-walled rotating pipes. Majidi et al. [36] studied the flutter analysis of trapezoidal plates reinforced by carbon nanotubes. Esmaeili et al. [37] performed the vibration analysis of composite laminated doubly curved shells reinforced by graphene platelets. An and Sun [38] researched the aeroelastic behaviours of cylindrical composite panels. Ye et al. [39] inspected the aeroelastic analysis of the viscoelastic panel. Rahmanian and Javadi [40] studied the dynamic instability of cylindrical shells made of FG porous material. Adamian et al. [41] investigated the vibration characteristics of a doubly curved panel reinforced by graphene nanoplatelets. The flutter behaviour of cylindrical panels reinforced by the graphene platelets was researched by Zhou et al. [42]. The parameter studies are carried out, revealing the influences of the pore, and graphene platelets on the flutter behaviour of the cylindrical panels. The dynamic instability of doubly curved shells reinforced with functionally graded carbon nanotubes was researched by Amin Yazdi [43]. He showed that the influence of panel imperfection on flutter aerodynamic pressure is more considerable than functionally graded carbon nanotube volume fractions and distributions. Subramani et al. [44] performed the dynamic characteristics of the spherical sandwich shell panel with carbon nanotubes reinforced. Majidi et al. [45] investigated the aeroelastic behaviour of spinning cylindrical shells composed of functionally graded material reinforced with graphene nanoplatelets using the first-order shear deformation theory. Abdollahi et al. [46] performed the aeroelastic analysis of trapezoidal sandwich plates with functionally graded porous face sheets and honeycomb cores in supersonic airflow. Merdaci et al. [47] studied the dynamic response of plates with various porosity distributions. Houshangi et al. [48] studied the flutter analysis of sandwich conical shells. Chen et al. [49] inspected the aeroelastic behaviour of composite plates surrounded by a piezoelectric layer. Arani et al. [50] researched the supersonic flutter behaviour of sandwich plates. Khorshidi et al. [51] investigated the vibration and stability of rectangular plates in contact with sloshing fluid on one side and under supersonic aeroelastic load on the other side.

Piezoelectric materials are the best choice for use in intelligent mechanical structures in the future due to their coupling mechanical and electrical properties. This is because there is a coupling between the mechanical and electrical properties of the piezoelectric material. In addition, lightweight and ductility are also special properties of these materials. Many researchers have studied the use of these materials in structures under fluid flow. Crawley and Luis [52] investigated the use of piezoelectric materials in intelligent structures. Zhou et al. [53] derived the flutter aerodynamics pressure for isotropic plates with piezoelectric layers. Song et al. [54] studied the flutter boundaries of the composite laminated plates with the piezoelectric layer. Li. [55] investigated
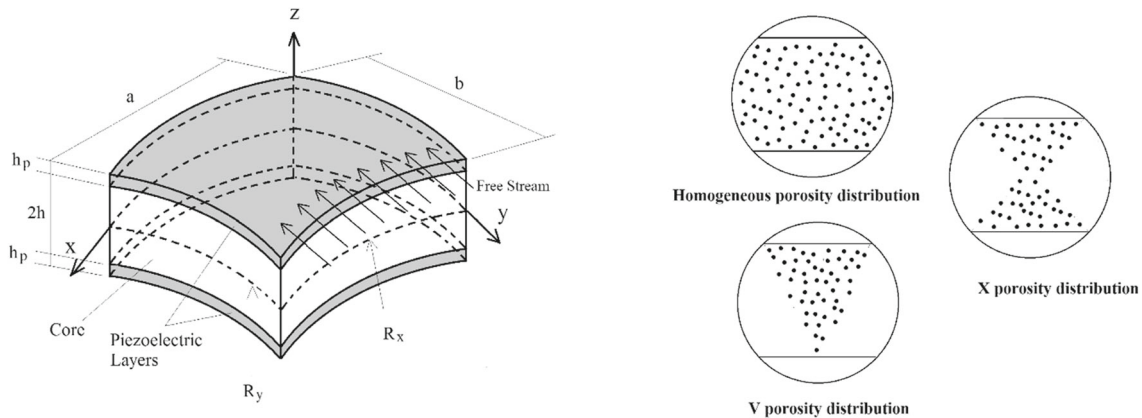
Fig. 1 Coordinate system and geometry of a doubly curved panel and schematic of three types of porosity distribution

the influences of piezoelectric materials to improve the flutter characteristics of the plates. Tsushima and Su [56] investigated the aeroelastic instability of highly flexible piezoelectric wings. Li et al. [57] showed that the use of piezoelectric materials increases the flutter velocities of the supersonic beams. Xue et al. [58] inspected the flutter characteristics of plates made of functionally graded piezoelectric material (FGPM) in supersonic airflow. Wang et al. [59] studied the vibration of a plate surrounded by two piezoelectric layers. The vibration behaviour of FGM plates with piezoelectric layers was performed by Farsangi et al. [60]. Almedia et al. [61] studied the aeroelastic stability boundary of composite panels caused by the piezoelectric actuator. Zhang et al. [62] investigated the aerothermoelastic characteristics of composite panels with piezoelectric layers. Tian et al. [63] performed the nonlinear aeroelastic characteristics of a functionally graded piezoelectric material (FGPM) plate. Tham et al. [64] studied the vibration analysis of functionally graded carbon nanotube-reinforced composite (FG-CNTRC) doubly curved shallow shells surrounded by piezoelectric layers.

To the best of the author's knowledge, the piezoelectricity effects on the flutter analysis of the doubly curved panels have not been studied, yet. In this study, for the first time, the flutter boundaries for a doubly curved panel made of FG porous materials surrounded by piezoelectric layers subjected to supersonic flow have been investigated. The doubly curved shell analysis has the feature that by changing the radius of curvature, analyses of cylindrical shell, spherical shell, and plate can be performed. In this regard, considering Reddy's third-order shear deformation theory and first-order piston theory, the governing equations of motion are obtained using Hamilton's principle and Maxwell's equation. The Galerkin method is used to discretize the equations of motion. To study the effects of piezoelectricity, three types of piezoelectric layers are investigated in both open-circuit and closed-circuit electrical boundary conditions. Also, the FG porous material with three types of porosity structure including uniform distribution, X-shaped distribution, and V-shaped distribution is investigated. Moreover, the effect of the power of the FG porous material and the porosity coefficient on the frequencies and the flutter boundaries are investigated. Flutter frequencies and flutter boundaries are compared for spherical, cylindrical, doubly curved shell with $R_y = -R_x$ and plate. Finally, the effects of mechanical boundary conditions, geometric parameters, and radii of curvatures of the middle surface on the flutter boundaries and flutter frequencies of FG porous doubly curved panels are investigated in detail. The results show that increasing the porosity coefficient reduces the stable range. Furthermore, open circuit electrical conditions cover a larger stable range. Also, using PZ4 piezoelectric layers results in the highest flutter boundaries and frequencies.

2 Mathematical formulation

Figure 1, shows the FG porous doubly curved panel with length a, width b, and total thickness $H = 2(h + h_p)$ where $2h$ and h_p are thickness of FG porous core and the thickness of each piezoelectric layers, respectively.

The radii of principal curvatures of the middle surface are assumed to be R_x and R_y. The Cartesian coordinate system is used. Based on Reddy's third-order shear deformation theory assumptions for doubly curved

panels, consistent the mid-surface displacements *(u, v, w)*, mid-surface rotations $\left(\psi_x, \psi_y\right)$, and displacements on a generic point of the panel $\left(u_x, u_y, u_z\right)$ are the association as (Reddy [65]):

$$u_x(x, y, z, t) = \left(1 + \frac{z}{R_x}\right)u(x, y, t) + z\psi_x(x, y, t) - cz^3\left(\psi_x(x, y, t) + \frac{\partial w(x, y, t)}{\partial x}\right)$$

$$u_y(x, y, z, t) = \left(1 + \frac{z}{R_y}\right)v(x, y, t) + z\psi_y(x, y, t) - cz^3\left(\psi_y(x, y, t) + \frac{\partial w(x, y, t)}{\partial y}\right)$$

$$u_z(x, y, z, t) = w(x, y, t) \tag{1}$$

where t stands for the time variable. The constant c is given by $c = \left(\frac{4}{3H^2}\right)$, which is obtained by satisfying the shear-free boundary conditions on the top and bottom surfaces of the shell as follows: (Reddy. [65], Murakami [70], Sciuva [71]).

$$\sigma_{xz}\big|_{z=\pm\frac{H}{2}} = 0, \sigma_{yz}\big|_{z=\pm\frac{H}{2}} = 0 \tag{2}$$

The linear strain–displacement relations are obtained as follows:

$$\varepsilon_{xx} = \left(\frac{\partial u}{\partial x} + \frac{w}{R_x}\right) + z\frac{\partial \psi_x}{\partial x} - cz^3\left(\frac{\partial \psi_x}{\partial x} + \frac{\partial^2 w}{\partial x^2} - \frac{\partial u}{R_x \partial x}\right)$$

$$\varepsilon_{yy} = \left(\frac{\partial v}{\partial y} + \frac{w}{R_y}\right) + z\frac{\partial \psi_y}{\partial y} - cz^3\left(\frac{\partial \psi_y}{\partial y} + \frac{\partial^2 w}{\partial y^2} - \frac{\partial v}{R_y \partial y}\right)$$

$$\varepsilon_{zz} = 0$$

$$\gamma_{xy} = 2\varepsilon_{xy} = \left(\frac{\partial u}{\partial y} + \frac{\partial v}{\partial x}\right) + z\left(\frac{\partial \psi_x}{\partial y} + \frac{\partial \psi_y}{\partial x}\right)$$

$$- cz^3\left(\frac{\partial \psi_x}{\partial y} + \frac{\partial \psi_y}{\partial x} + 2\frac{\partial^2 w}{\partial x \partial y} - \frac{\partial u}{R_x \partial x} - \frac{\partial v}{R_y \partial y}\right)$$

$$\gamma_{xz} = 2\varepsilon_{xz} = \left(1 - \beta z^2\right)\left(\psi_x + \frac{\partial w}{\partial x} - \frac{u}{R_x}\right)$$

$$\gamma_{yz} = 2\varepsilon_{yz} = \left(1 - \beta z^2\right)\left(\psi_y + \frac{\partial w}{\partial y} - \frac{v}{R_y}\right) \tag{3}$$

Here, ε_{xx} and ε_{yy} are the normal strains; γ_{xy}, γ_{xz} and γ_{yz} are the shear strains and the constant β is defined as:

$$\beta = 3c = \frac{4}{H^2} \tag{4}$$

The stress components are expressed as:

$$\begin{Bmatrix} \sigma_{xx} \\ \sigma_{yy} \\ \sigma_{xy} \\ \sigma_{xz} \\ \sigma_{yz} \end{Bmatrix} = \begin{bmatrix} Q_{11} & Q_{12} & 0 & 0 & 0 \\ Q_{12} & Q_{22} & 0 & 0 & 0 \\ 0 & 0 & Q_{66} & 0 & 0 \\ 0 & 0 & 0 & Q_{55} & 0 \\ 0 & 0 & 0 & 0 & Q_{44} \end{bmatrix} \begin{Bmatrix} \varepsilon_{xx} \\ \varepsilon_{yy} \\ 2\varepsilon_{xy} \\ 2\varepsilon_{xz} \\ 2\varepsilon_{yz} \end{Bmatrix} \tag{5}$$

These are defined as:

$$Q_{11} = Q_{22} = \frac{E(z)}{1 - \upsilon^2}$$

$$Q_{12} = Q_{21} = \frac{\upsilon E(z)}{1 - \upsilon^2}$$

$$Q_{44} = Q_{55} = Q_{66} = \frac{1}{2}(Q_{11} - Q_{12}) = \frac{E(z)}{2(1 + \upsilon)} \tag{6}$$

The properties of FG porous layers can be written as:

$$P = P_b + (P_t - P_b)\left(\frac{z+h}{2h}\right)^n - \frac{e}{2}(P_t + P_b) \quad \text{homogeneous distribution} \tag{7.a}$$

$$P = P_b + (P_t - P_b)\left(\frac{z+h}{2h}\right)^n - \frac{e}{2}(P_t + P_b)\left(\left|\frac{h-2z}{2h}\right|\right) \quad \text{V distribution} \tag{7.b}$$

$$P = P_b + (P_t - P_b)\left(\frac{z+h}{2h}\right)^n - \frac{e}{2}(P_t + P_b)\left(\left|\frac{2z}{h}\right|\right) \quad \text{X distribution} \tag{7.c}$$

The forms of porosity distribution for homogeneous, V and X distribution are given in Fig. 1. Equation (7.a) shows the homogeneous distribution of porosity, Eq. (7.b) shows that the porosity distribution is V type, and Eq. (7.c) shows that the porosity distribution is X type. In Eq. (7), P represents the property of the material, e, and n represents the porosity and power law index.

Also, P_b and P_t represent the material properties on the bottom and top surfaces of the panel, respectively. (Ebrahimi and Jafari [66], Wattanasakulpong and Ungbhakorn [68]). In the present research, the materials on the bottom and top surfaces of the shell are ceramics and metal, respectively.

The constitutive equation for the piezoelectric materials is expressed as Eq. (8). (Wang et al. [59]).

$$\begin{Bmatrix} \sigma_{xx} \\ \sigma_{yy} \\ \sigma_{yz} \\ \sigma_{xz} \\ \sigma_{xy} \end{Bmatrix} = \begin{bmatrix} \bar{c}_{11} & \bar{c}_{12} & 0 & 0 & 0 \\ \bar{c}_{12} & \bar{c}_{11} & 0 & 0 & 0 \\ 0 & 0 & c_{55} & 0 & 0 \\ 0 & 0 & 0 & c_{55} & 0 \\ 0 & 0 & 0 & 0 & (\bar{c}_{11}-\bar{c}_{12})/2 \end{bmatrix} \begin{Bmatrix} \varepsilon_{xx} \\ \varepsilon_{yy} \\ \gamma_{yz} \\ \gamma_{xz} \\ \gamma_{xy} \end{Bmatrix} - \begin{bmatrix} 0 & 0 & \bar{e}_{31} \\ 0 & 0 & \bar{e}_{31} \\ 0 & e_{15} & 0 \\ e_{15} & 0 & 0 \\ 0 & 0 & 0 \end{bmatrix} \begin{Bmatrix} E_x \\ E_y \\ E_z \end{Bmatrix} \tag{8}$$

$$\begin{Bmatrix} D_x \\ D_y \\ D_z \end{Bmatrix} = \begin{bmatrix} 0 & 0 & 0 & e_{15} & 0 \\ 0 & 0 & e_{15} & 0 & 0 \\ \bar{e}_{31} & \bar{e}_{31} & 0 & 0 & 0 \end{bmatrix} \begin{Bmatrix} \varepsilon_{xx} \\ \varepsilon_{yy} \\ \gamma_{yz} \\ \gamma_{xz} \\ \gamma_{xy} \end{Bmatrix} + \begin{bmatrix} \Xi_{11} & 0 & 0 \\ 0 & \Xi_{11} & 0 \\ 0 & 0 & \bar{\Xi}_{33} \end{bmatrix} \begin{Bmatrix} E_x \\ E_y \\ E_z \end{Bmatrix} \tag{9}$$

In which

$$\bar{c}_{11} = c_{11} - \frac{c_{13}^2}{c_{33}}, \quad \bar{c}_{12} = c_{12} - \frac{c_{13}^2}{c_{33}}$$

$$\bar{e}_{31} = e_{31} - \frac{c_{13}}{c_{33}}e_{33}, \quad \bar{\Xi}_{33} = \Xi_{33} + \frac{e_{33}^2}{c_{33}} \tag{10}$$

In Eq. (9), the electrical displacement and electric field in the piezoelectric layer are denoted by D_i and E_i ($i = x, y, z$) respectively. Besides, $c_{11}, c_{12}, c_{13}, c_{33}$ and c_{55} are piezoelectric elastic moduli; e_{31}, e_{33} and e_{15} are piezoelectric constant and Ξ_{11}, and Ξ_{33} are dielectric permittivity.

The electric field can be expressed as Eq. (11). So that Φ is the electric potential.

$$E_x = -\frac{\partial \Phi}{\partial x}, \quad E_y = -\frac{\partial \Phi}{\partial y}, \quad E_z = -\frac{\partial \Phi}{\partial z} \tag{11}$$

In Eq. (12), Φ is defined for closed circuit conditions where $\phi(x, y, t)$ is the electric potential in the mid-surface of piezoelectric layers.

$$\Phi(x, y, z, t) = \begin{cases} \phi(x, y, t)\left[1 - \left(\frac{z-h-h_p/2}{h_p/2}\right)^2\right] & (h \leq z \leq h + h_p) \\ \phi(x, y, t)\left[1 - \left(\frac{-z-h-h_p/2}{h_p/2}\right)^2\right] & (-h - h_p \leq z \leq -h) \end{cases} \tag{12}$$

The electric potential function for open circuit condition is expressed as

$$
\Phi(x,y,z,t) =
\begin{cases}
\phi(x,y,t)\left[1-\left(\dfrac{z-h-h_p/2}{h_p/2}\right)^2+\dfrac{4(z-h)}{h_p}\right] \\
+\dfrac{\overline{e}_{31}}{\overline{\Xi}_{33}}\left\{
\begin{array}{l}
\dfrac{\partial u}{\partial x}+\dfrac{w}{R_x}+\dfrac{\partial v}{\partial y}+\dfrac{w}{R_y}+\left[h+h_p-c\left(h+h_p\right)^3\right]\left(\dfrac{\partial \psi_x}{\partial x}-\dfrac{\partial u}{R_x\partial x}+\dfrac{\partial \psi_y}{\partial y}-\dfrac{\partial v}{R_y\partial y}\right) \\
-c\left(h+h_p\right)^3\nabla^2 w
\end{array}\right\}(z-h) & \left(h\le z\le h+h_p\right) \\[6pt]
\phi(x,y,t)\left[1-\left(\dfrac{-z-h-h_p/2}{h_p/2}\right)^2-\dfrac{4(z+h)}{h_p}\right] \\
+\dfrac{\overline{e}_{31}}{\overline{\Xi}_{33}}\left\{
\begin{array}{l}
\dfrac{\partial u}{\partial x}+\dfrac{w}{R_x}+\dfrac{\partial v}{\partial y}+\dfrac{w}{R_y}-\left[h+h_p-c\left(h+h_p\right)^3\right]\left(\dfrac{\partial \psi_x}{\partial x}-\dfrac{\partial u}{R_x\partial x}+\dfrac{\partial \psi_y}{\partial y}-\dfrac{\partial v}{R_y\partial y}\right) \\
+c\left(h+h_p\right)^3\nabla^2 w
\end{array}\right\}(z+h) & \left(-h-h_p\le z\le -h\right)
\end{cases}
$$
$$(13)$$

According to the first-order piston theory, the aerodynamic pressure load is expressed as (Dowell. [67])

$$
\Delta P = -\frac{\rho_\infty U_\infty^2}{\sqrt{M_\infty^2-1}}\left(\frac{\partial w(x,y,t)}{\partial x}+\frac{M_\infty^2-2}{M_\infty^2-1}\frac{1}{U_\infty}\frac{\partial w(x,y,t)}{\partial t}\right) \tag{14}
$$

where, M_∞, U_∞ and ρ_∞ represent the Mach number, velocity, and density of airflow, respectively. The following simplification for high Mach numbers is utilized: (Dowell [67])

$$
\frac{M_\infty^2-2}{M_\infty^2-1}\left(\frac{\mu}{\lambda\sqrt{M_\infty^2-1}}\right)^{1/2}=\left(\frac{\mu}{\lambda M_\infty}\right)^{1/2} \tag{15.a}
$$

$$
\lambda=\frac{\rho_\infty U_\infty^2 a^3}{D_m\sqrt{M_\infty^2-1}},\mu=\frac{\rho_\infty a}{2\rho_t h} \tag{15.b}
$$

where, λ is the non-dimension aerodynamic pressure.

Based on Hamilton's principle, the governing equations are obtained as

$$
\int_{t_1}^{t_2}(\delta T-\delta U-\delta V)dt=0 \tag{16}
$$

In Eq. (16), the variational form of strain energy, kinetic energy, and virtual work of an aeroelastic force is demonstrated by δU, δT and δV, respectively. So that, they can be expressed as

$$
\delta U=\iint_A\int_{-h-h_p}^{h+h_p}\left\{\sigma_{xx}\delta\varepsilon_{xx}+\sigma_{yy}\delta\varepsilon_{yy}+\sigma_{zz}\delta\varepsilon_{zz}+\sigma_{xy}\delta\gamma_{xy}+\sigma_{xz}\delta\gamma_{xz}+\sigma_{yz}\delta\gamma_{yz}\right\}dAdz \tag{17}
$$

$$
\begin{aligned}
\int_{t_1}^{t_2}\delta T dt=-\int_{t_1}^{t_2}\iint_A\Big\{&\left[\left(I_0+\frac{2}{R_x}I_1+\frac{1}{R_x^2}I_2\right)\frac{\partial^2 u}{\partial t^2}+\left(I_1+\frac{1}{R_x}I_2-c\left(I_3+\frac{1}{R_x}I_4\right)\right)\frac{\partial^2\psi_x}{\partial t^2}-c\left(I_3+\frac{1}{R_x}I_4\right)\frac{\partial^3 w}{\partial x\partial t^2}\right]\delta u \\
&+\left[\left(I_0+\frac{2}{R_y}I_1+\frac{1}{R_y^2}I_2\right)\frac{\partial^2 v}{\partial t^2}+\left(I_1+\frac{1}{R_y}I_2-c\left(I_3+\frac{1}{R_y}I_4\right)\right)\frac{\partial^2\psi_y}{\partial t^2}-c\left(I_3+\frac{1}{R_y}I_4\right)\frac{\partial^3 w}{\partial y\partial t^2}\right]\delta v \\
&+\left[\left(I_1+\frac{1}{R_x}I_2-cI_3-\frac{c}{R_x}I_4\right)\frac{\partial^2 u}{\partial t^2}+\left(I_2-2cI_4+c^2 I_6\right)\frac{\partial^2\psi_x}{\partial t^2}+\left(-cI_4+c^2 I_6\right)\frac{\partial^3 w}{\partial x\partial t^2}\right]\delta\psi_x \\
&+\left[\left(I_1+\frac{I_2}{R_y}-cI_3-c\frac{I_4}{R_y}\right)\frac{\partial^2 v}{\partial t^2}+\left(I_2-2cI_4+c^2 I_6\right)\frac{\partial^2\psi_y}{\partial t^2}+\left(-cI_4+c^2 I_6\right)\frac{\partial^3 w}{\partial y\partial t^2}\right]\delta\psi_y \\
&+\left[I_0\frac{\partial^2 w}{\partial t^2}-c\left[\left(I_3+\frac{I_4}{R_x}\right)\left(\frac{\partial^3 u}{\partial x\partial t^2}\right)+\left(I_3+\frac{I_4}{R_y}\right)\left(\frac{\partial^3 v}{\partial y\partial t^2}\right)+\left(I_4-cI_6\right)\left(\frac{\partial^3\psi_x}{\partial x\partial t^2}\right)\right.\right. \\
&\left.\left.+\left(I_4-cI_6\right)\left(\frac{\partial^3\psi_y}{\partial y\partial t^2}\right)-cI_6\left(\frac{\partial^4 w}{\partial x^2\partial t^2}+\frac{\partial^4 w}{\partial y^2\partial t^2}\right)\right]\right]\delta w\Big\}dA
\end{aligned} \tag{18}
$$

The virtual work of aeroelastic forces (δV) can be represented as:

$$\delta V = \int\limits_{-h-h_p}^{h+h_p} \Delta P \delta w \, dz \tag{19}$$

Substituting Eqs. (17), (18) and (19) into Hamilton's principle, the governing equations of motion are derived as:

$$\delta u : \frac{\partial N_{xx}}{\partial x} + \frac{\partial N_{xy}}{\partial y} + \frac{c}{R_x}\left(\frac{\partial S_{xx}}{\partial x} + \frac{\partial S_{xy}}{\partial y}\right) + \frac{\beta}{R_x} P_x - \frac{1}{R_x} Q_x$$

$$= \left(I_0 + \frac{2}{R_x} I_1 + \frac{1}{R_x^2} I_2\right)\frac{\partial^2 u}{\partial t^2} + \left(I_1 + \frac{1}{R_x} I_2 - c\left(I_3 + \frac{1}{R_x} I_4\right)\right)\frac{\partial^2 \psi_x}{\partial t^2} - c\left(I_3 + \frac{1}{R_x} I_4\right)\frac{\partial^3 w}{\partial x \partial t^2} \tag{20.a}$$

$$\delta v : \frac{\partial N_{yy}}{\partial y} + \frac{\partial N_{xy}}{\partial x} + \frac{c}{R_y}\left(\frac{\partial S_{yy}}{\partial y} + \frac{\partial S_{xy}}{\partial x}\right) + \frac{\beta}{R_y} P_y - \frac{1}{R_y} Q_y$$

$$= \left(I_0 + \frac{2}{R_y} I_1 + \frac{1}{R_y^2} I_2\right)\frac{\partial^2 v}{\partial t^2} + \left(I_1 + \frac{1}{R_y} I_2 - c\left(I_3 + \frac{1}{R_y} I_4\right)\right)\frac{\partial^2 \psi_y}{\partial t^2} - c\left(I_3 + \frac{1}{R_y} I_4\right)\frac{\partial^3 w}{\partial y \partial t^2} \tag{20.b}$$

$$\delta \psi_x : \frac{\partial M_{xx}}{\partial x} + \frac{\partial M_{xy}}{\partial y} - c\left(\frac{\partial S_{xx}}{\partial x} + \frac{\partial S_{xy}}{\partial y}\right) + Q_x - \beta P_x$$

$$= \left(I_1 + \frac{1}{R_x} I_2 - c I_3 - \frac{c}{R_x} I_4\right)\frac{\partial^2 u}{\partial t^2} + \left(I_2 - 2c I_4 + c^2 I_6\right)\frac{\partial^2 \psi_x}{\partial t^2} + \left(-c I_4 + c^2 I_6\right)\frac{\partial^3 w}{\partial x \partial t^2} \tag{20.c}$$

$$\delta \psi_y : \frac{\partial M_{xy}}{\partial x} + \frac{\partial M_{yy}}{\partial y} - c\left(\frac{\partial S_{xy}}{\partial x} + \frac{\partial S_{yy}}{\partial y}\right) + Q_y - \beta P_y$$

$$= \left(I_1 + \frac{I_2}{R_y} - c I_3 - c\frac{I_4}{R_y}\right)\frac{\partial^2 v}{\partial t^2} + \left(I_2 - 2c I_4 + c^2 I_6\right)\frac{\partial^2 \psi_y}{\partial t^2} + \left(-c I_4 + c^2 I_6\right)\frac{\partial^3 w}{\partial y \partial t^2} \tag{20.d}$$

$$\delta w : \frac{\partial Q_x}{\partial x} + \frac{\partial Q_y}{\partial y} + \frac{N_{xx}}{R_x} + \frac{N_{yy}}{R_y} - c\left(\frac{\partial^2 S_{xx}}{\partial x^2} + \frac{\partial^2 S_{yy}}{\partial y^2} + 2\frac{\partial^2 S_{xy}}{\partial x \partial y}\right) - \beta\left(\frac{\partial P_x}{\partial x} + \frac{\partial P_y}{\partial y}\right) + \Delta P$$

$$= I_0 \frac{\partial^2 w}{\partial t^2} - c\left[\left(I_3 + \frac{I_4}{R_x}\right)\left(\frac{\partial^3 u}{\partial x \partial t^2}\right) + \left(I_3 + \frac{I_4}{R_y}\right)\left(\frac{\partial^3 v}{\partial y \partial t^2}\right)\right.$$

$$\left. + \left(I_4 - c I_6\right)\left(\frac{\partial^3 \psi_x}{\partial x \partial t^2}\right) + \left(I_4 - c I_6\right)\left(\frac{\partial^3 \psi_y}{\partial y \partial t^2}\right) - c I_6\left(\frac{\partial^4 w}{\partial x^2 \partial t^2} + \frac{\partial^4 w}{\partial y^2 \partial t^2}\right)\right] \tag{20.e}$$

In Eq. (20), the forces and moments resultants can be defined as

$$N_{xx} = A_{11}\left(\frac{\partial u}{\partial x} + \frac{w}{R_x}\right) + A_{12}\left(\frac{\partial v}{\partial y} + \frac{w}{R_y}\right) + B_{11}\frac{\partial \psi_x}{\partial x} + B_{12}\frac{\partial \psi_y}{\partial y}$$

$$- c F_{11}\left(\frac{\partial \psi_x}{\partial y} + \frac{\partial^2 w}{\partial x^2} - \frac{\partial u}{R_x \partial x}\right) - c F_{11}\left(\frac{\partial \psi_y}{\partial y} + \frac{\partial^2 w}{\partial y^2} - \frac{\partial v}{R_y \partial y}\right) + T_1 \varphi$$

$$N_{yy} = A_{21}\left(\frac{\partial u}{\partial x} + \frac{w}{R_x}\right) + A_{22}\left(\frac{\partial v}{\partial y} + \frac{w}{R_y}\right) + B_{21}\frac{\partial \psi_x}{\partial x} + B_{22}\frac{\partial \psi_y}{\partial y}$$

$$- c F_{21}\left(\frac{\partial \psi_x}{\partial y} + \frac{\partial^2 w}{\partial x^2} - \frac{\partial u}{R_x \partial x}\right) - c F_{22}\left(\frac{\partial \psi_y}{\partial y} + \frac{\partial^2 w}{\partial y^2} - \frac{\partial v}{R_y \partial y}\right) + T_1 \varphi$$

$$N_{xy} = A_{66}\left(\frac{\partial u}{\partial y} + \frac{\partial v}{\partial x}\right) + B_{66}\left(\frac{\partial \psi_x}{\partial y} + \frac{\partial \psi_y}{\partial x}\right) - c F_{66}\left(\frac{\partial \psi_x}{\partial y} + \frac{\partial \psi_y}{\partial x} + 2\frac{\partial^2 w}{\partial x \partial y} - \frac{\partial u}{R_x \partial y} - \frac{\partial v}{R_y \partial x}\right)$$

$$M_{xx} = B_{11}\left(\frac{\partial u}{\partial x} + \frac{w}{R_x}\right) + B_{12}\left(\frac{\partial v}{\partial y} + \frac{w}{R_y}\right) + D_{11}\frac{\partial \psi_x}{\partial x} + D_{12}\frac{\partial \psi_y}{\partial y}$$

$$- c G_{11}\left(\frac{\partial \psi_x}{\partial x} + \frac{\partial^2 w}{\partial x^2} - \frac{\partial u}{R_x \partial x}\right) - c G_{12}\left(\frac{\partial \psi_y}{\partial y} + \frac{\partial^2 w}{\partial y^2} - \frac{\partial v}{R_y \partial y}\right) + \bar{T}_1 \varphi$$

$$M_{yy} = B_{11}\left(\frac{\partial u}{\partial x} + \frac{w}{R_x}\right) + B_{12}\left(\frac{\partial v}{\partial y} + \frac{w}{R_y}\right) + D_{11}\frac{\partial \psi_x}{\partial x} + D_{12}\frac{\partial \psi_y}{\partial y}$$

$$- cG_{11}\left(\frac{\partial \psi_x}{\partial x} + \frac{\partial^2 w}{\partial x^2} - \frac{\partial u}{R_x \partial x}\right) - cG_{12}\left(\frac{\partial \psi_y}{\partial y} + \frac{\partial^2 w}{\partial y^2} - \frac{\partial v}{R_y \partial y}\right) + \bar{T}_1 \varphi$$

$$M_{xy} = B_{66}\left(\frac{\partial u}{\partial y} + \frac{\partial v}{\partial x}\right) + D_{66}\left(\frac{\partial \psi_x}{\partial y} + \frac{\partial \psi_y}{\partial x}\right) - cG_{66}\left(\frac{\partial \psi_x}{\partial y} + \frac{\partial \psi_y}{\partial x} + 2\frac{\partial^2 w}{\partial x \partial y} - \frac{\partial u}{R_x \partial y} - \frac{\partial v}{R_y \partial x}\right)$$

$$Q_x = A_{55}\left(\psi_x + \frac{\partial w}{\partial x} - \frac{u}{R_x}\right) + T_5\frac{\partial \phi}{\partial x}$$

$$Q_y = A_{44}\left(\psi_y + \frac{\partial w}{\partial y} - \frac{v}{R_y}\right) + T_5\frac{\partial \phi}{\partial y}$$

$$S_{xx} = F_{11}\left(\frac{\partial u}{\partial x} + \frac{w}{R_x}\right) + F_{12}\left(\frac{\partial v}{\partial y} + \frac{w}{R_y}\right) + G_{11}\frac{\partial \psi_x}{\partial x} + G_{12}\frac{\partial \psi_y}{\partial y}$$

$$- cH_{11}\left(\frac{\partial \psi_x}{\partial x} + \frac{\partial^2 w}{\partial x^2} - \frac{\partial u}{R_x \partial x}\right) - cH_{12}\left(\frac{\partial \psi_y}{\partial y} + \frac{\partial^2 w}{\partial y^2} - \frac{\partial v}{R_y \partial y}\right) - \bar{T}_1 \phi$$

$$S_{yy} = F_{21}\left(\frac{\partial u}{\partial x} + \frac{w}{R_x}\right) + F_{22}\left(\frac{\partial v}{\partial y} + \frac{w}{R_y}\right) + G_{21}\frac{\partial \psi_x}{\partial x} + G_{22}\frac{\partial \psi_y}{\partial y}$$

$$- cH_{21}\left(\frac{\partial \psi_x}{\partial x} + \frac{\partial^2 w}{\partial x^2} - \frac{\partial u}{R_x \partial x}\right) - cH_{22}\left(\frac{\partial \psi_y}{\partial y} + \frac{\partial^2 w}{\partial y^2} - \frac{\partial v}{R_y \partial y}\right) - \bar{T}_1 \phi$$

$$S_{xy} = F_{66}\left(\frac{\partial u}{\partial y} + \frac{\partial v}{\partial x}\right) + G_{66}\left(\frac{\partial \psi_x}{\partial y} + \frac{\partial \psi_y}{\partial x}\right) - cH_{66}\left(\frac{\partial \psi_x}{\partial y} + \frac{\partial \psi_y}{\partial x} + 2\frac{\partial^2 w}{\partial x \partial y} - \frac{\partial u}{R_x \partial y} - \frac{\partial v}{R_y \partial x}\right)$$

$$P_x = -\beta\left(D_{55}\left(\psi_x + \frac{\partial w}{\partial x} - \frac{u}{R_x}\right) + \bar{T}_5 \phi\right)$$

$$P_y = -\beta\left(D_{44}\left(\psi_y + \frac{\partial w}{\partial y} - \frac{v}{R_y}\right) + \bar{T}_5 \phi\right) \tag{21}$$

Substituting Eq. (21) into Eq. (20), the governing equations can be presented as

$$\delta u : ab_1 \frac{\partial^2 u}{\partial x^2} + ab_2 \frac{\partial^2 u}{\partial y^2} + ab_3 u + ab_4 \frac{\partial^2 v}{\partial x \partial y} + ab_5 \frac{\partial^2 \psi_x}{\partial x^2} + ab_6 \frac{\partial^2 \psi_x}{\partial y^2} + ab_7 \psi_x + ab_8 \frac{\partial^2 \psi_y}{\partial x \partial y}$$

$$+ ab_9 \frac{\partial^3 w}{\partial x^3} + ab_{10} \frac{\partial^3 w}{\partial x \partial y^2} + ab_{11} \frac{\partial w}{\partial x} + T_2\left(\left(\frac{\partial^2 u}{\partial x^2} + \frac{\partial w}{R_x \partial x}\right) + \left(\frac{\partial^2 v}{\partial x \partial y} + \frac{\partial w}{R_y \partial x}\right)\right)$$

$$+ \frac{1}{R_x}\left(T_5\frac{\partial \phi}{\partial x} + T_7\left(\frac{\partial^2 \psi_x}{\partial x^2} + \frac{\partial^2 \psi_y}{\partial x \partial y}\right) + T_8\left(\frac{\partial^2 \psi_x}{\partial x^2} + \frac{\partial^3 w}{\partial x^3} - \frac{\partial^2 u}{R_x \partial x^2} + \frac{\partial^2 \psi_y}{\partial x \partial y} + \frac{\partial^3 w}{\partial x \partial y^2} - \frac{\partial^2 v}{R_y \partial x \partial y}\right)\right.$$

$$- \beta\left(T_{5z2}\frac{\partial \phi}{\partial x} + T_{7z2}\left(\frac{\partial^2 \psi_x}{\partial x^2} + \frac{\partial^2 \psi_y}{\partial x \partial y}\right) + T_{8z2}\left(\frac{\partial^2 \psi_x}{\partial x^2} + \frac{\partial^3 w}{\partial x^3} - \frac{\partial^2 u}{R_x \partial x^2} + \frac{\partial^2 \psi_y}{\partial x \partial y} + \frac{\partial^3 w}{\partial x \partial y^2} - \frac{\partial^2 v}{R_y \partial x \partial y}\right)\right)$$

$$+ \frac{c}{R_x}\left(T_{1z3}\frac{\partial \phi}{\partial x} + T_{3z3}\left(\frac{\partial^2 \psi_x}{\partial x^2} + \frac{\partial^2 \psi_y}{\partial x \partial y}\right) + T_{4z3}\left(\frac{\partial^2 \psi_x}{\partial x^2} + \frac{\partial^3 w}{\partial x^3} - \frac{\partial^2 u}{R_x \partial x^2} + \frac{\partial^2 \psi_y}{\partial x \partial y} + \frac{\partial^3 w}{\partial x \partial y^2} - \frac{\partial^2 v}{R_y \partial x \partial y}\right)\right)$$

$$= \left(I_0 + \frac{2}{R_x}I_1 + \frac{1}{R_x^2}I_2\right)\frac{\partial^2 u}{\partial t^2} + \left(I_1 + \frac{1}{R_x}I_2 - c\left(I_3 + \frac{1}{R_x}I_4\right)\right)\frac{\partial^2 \psi_x}{\partial t^2} - c\left(I_3 + \frac{1}{R_x}I_4\right)\frac{\partial^3 w}{\partial x \partial t^2}$$

$$\tag{22.a}$$

$$\delta v : ac_1 \frac{\partial^2 u}{\partial x \partial y} + ac_2 \frac{\partial^2 v}{\partial x^2} + ac_3 \frac{\partial^2 v}{\partial y^2} + ac_4 v + ac_5 \frac{\partial^2 \psi_x}{\partial x \partial y} + ac_6 \frac{\partial^2 \psi_y}{\partial x^2} + ac_7 \frac{\partial^2 \psi_y}{\partial y^2} + ac_8 \psi_y$$

$$+ ac_9 \frac{\partial^3 w}{\partial x^2 \partial y} + ac_{10} \frac{\partial^3 w}{\partial y^3} + ac_{11} \frac{\partial w}{\partial y} + T_2 \left(\left(\frac{\partial^2 u}{\partial x \partial y} + \frac{\partial w}{R_x \partial y} \right) + \left(\frac{\partial^2 v}{\partial y^2} + \frac{\partial w}{R_y \partial y} \right) \right)$$

$$+ \frac{1}{R_y} \left(T_5 \frac{\partial \phi}{\partial y} + T_7 \left(\frac{\partial^2 \psi_x}{\partial x \partial y} + \frac{\partial^2 \psi_y}{\partial y^2} \right) + T_8 \left(\frac{\partial^2 \psi_x}{\partial x \partial y} + \frac{\partial^3 w}{\partial x^2 \partial y} - \frac{\partial^2 u}{R_x \partial x \partial y} + \frac{\partial^2 \psi_y}{\partial y^2} + \frac{\partial^3 w}{\partial y^3} - \frac{\partial^2 v}{R_y \partial y^2} \right) \right.$$

$$\left. - \beta \left(T_{5z2} \frac{\partial \phi}{\partial y} + T_{7z2} \left(\frac{\partial^2 \psi_x}{\partial x \partial y} + \frac{\partial^2 \psi_y}{\partial y^2} \right) + T_{8z2} \left(\frac{\partial^2 \psi_x}{\partial x \partial y} + \frac{\partial^3 w}{\partial x^2 \partial y} - \frac{\partial^2 u}{R_x \partial x \partial y} + \frac{\partial^2 \psi_y}{\partial y^2} + \frac{\partial^3 w}{\partial y^3} - \frac{\partial^2 v}{R_y \partial y^2} \right) \right) \right)$$

$$+ \frac{c}{R_y} \left(T_{1z3} \frac{\partial \phi}{\partial y} + T_{3z3} \left(\frac{\partial^2 \psi_x}{\partial x \partial y} + \frac{\partial^2 \psi_y}{\partial y^2} \right) + T_{4z3} \left(\frac{\partial^2 \psi_x}{\partial x \partial y} + \frac{\partial^3 w}{\partial x^2 \partial y} - \frac{\partial^2 u}{R_x \partial x \partial y} + \frac{\partial^2 \psi_y}{\partial y^2} + \frac{\partial^3 w}{\partial y^3} - \frac{\partial^2 v}{R_y \partial y^2} \right) \right)$$

$$= \left(I_0 + \frac{2}{R_y} I_1 + \frac{1}{R_y^2} I_2 \right) \frac{\partial^2 v}{\partial t^2} + \left(I_1 + \frac{1}{R_y} I_2 - c \left(I_3 + \frac{1}{R_y} I_4 \right) \right) \frac{\partial^2 \psi_y}{\partial t^2} - c \left(I_3 + \frac{1}{R_y} I_4 \right) \frac{\partial^3 w}{\partial y \partial t^2}$$

$$(22.b)$$

$$\delta \psi_x : ad_1 \frac{\partial^2 u}{\partial x^2} + ad_2 \frac{\partial^2 u}{\partial y^2} + ad_3 u + ad_4 \frac{\partial^2 v}{\partial x \partial y} + ad_5 \frac{\partial^2 \psi_x}{\partial x^2} + ad_6 \psi_x$$

$$+ ad_7 \frac{\partial^2 \psi_x}{\partial y^2} + ad_8 \frac{\partial^2 \psi_y}{\partial x \partial y} + ad_9 \frac{\partial^3 w}{\partial x^3} + ad_{10} \frac{\partial^3 w}{\partial x \partial y^2} + ad_{11} \frac{\partial w}{\partial x}$$

$$+ \left(T_{1z} \frac{\partial \phi}{\partial x} + T_{3z} \left(\frac{\partial^2 \psi_x}{\partial x^2} + \frac{\partial^2 \psi_y}{\partial x \partial y} \right) + T_{4z} \left(\frac{\partial^2 \psi_x}{\partial x^2} + \frac{\partial^3 w}{\partial x^3} - \frac{\partial^2 u}{R_x \partial x^2} + \frac{\partial^2 \psi_y}{\partial x \partial y} + \frac{\partial^3 w}{\partial x \partial y^2} - \frac{\partial^2 v}{R_y \partial x \partial y} \right) \right.$$

$$\left. - \left(T_5 \frac{\partial \phi}{\partial x} + T_7 \left(\frac{\partial^2 \psi_x}{\partial x^2} + \frac{\partial^2 \psi_y}{\partial x \partial y} \right) + T_8 \left(\frac{\partial^2 \psi_x}{\partial x^2} + \frac{\partial^3 w}{\partial x^3} - \frac{\partial^2 u}{R_x \partial x^2} + \frac{\partial^2 \psi_y}{\partial x \partial y} + \frac{\partial^3 w}{\partial x \partial y^2} - \frac{\partial^2 v}{R_y \partial x \partial y} \right) \right) \right)$$

$$- \beta \left(T_{5z2} \frac{\partial \phi}{\partial x} + T_{7z2} \left(\frac{\partial^2 \psi_x}{\partial x^2} + \frac{\partial^2 \psi_y}{\partial x \partial y} \right) + T_{8z2} \left(\frac{\partial^2 \psi_x}{\partial x^2} + \frac{\partial^3 w}{\partial x^3} - \frac{\partial^2 u}{R_x \partial x^2} + \frac{\partial^2 \psi_y}{\partial x \partial y} + \frac{\partial^3 w}{\partial x \partial y^2} - \frac{\partial^2 v}{R_y \partial x \partial y} \right) \right)$$

$$- c \left(T_{1z3} \frac{\partial \phi}{\partial x} + T_{3z3} \left(\frac{\partial^2 \psi_x}{\partial x^2} + \frac{\partial^2 \psi_y}{\partial x \partial y} \right) + T_{4z3} \left(\frac{\partial^2 \psi_x}{\partial x^2} + \frac{\partial^3 w}{\partial x^3} - \frac{\partial^2 u}{R_x \partial x^2} + \frac{\partial^2 \psi_y}{\partial x \partial y} + \frac{\partial^3 w}{\partial x \partial y^2} - \frac{\partial^2 v}{R_y \partial x \partial y} \right) \right)$$

$$= \left(I_1 + \frac{1}{R_x} I_2 - c I_3 - \frac{c}{R_x} I_4 \right) \frac{\partial^2 u}{\partial t^2} + \left(I_2 - 2c I_4 + c^2 I_6 \right) \frac{\partial^2 \psi_x}{\partial t^2} + \left(-c I_4 + c^2 I_6 \right) \frac{\partial^3 w}{\partial x \partial t^2}$$

$$(22.c)$$

$$\delta \psi_y : af_1 \frac{\partial^2 u}{\partial x \partial y} + af_2 \frac{\partial^2 v}{\partial x^2} + af_3 \frac{\partial^2 v}{\partial y^2} + af_4 v + af_5 \frac{\partial^2 \psi_x}{\partial x \partial y} + af_6 \frac{\partial^2 \psi_y}{\partial x^2}$$

$$+ af_7 \frac{\partial^2 \psi_y}{\partial y^2} + af_8 \psi_y + af_9 \frac{\partial^3 w}{\partial x^2 \partial y} + af_{10} \frac{\partial^3 w}{\partial y^3} + af_{11} \frac{\partial w}{\partial y}$$

$$+ \left(T_{1z} \frac{\partial \phi}{\partial y} + T_{3z} \left(\frac{\partial^2 \psi_x}{\partial x \partial y} + \frac{\partial^2 \psi_y}{\partial y^2} \right) + T_{4z} \left(\frac{\partial^2 \psi_x}{\partial x \partial y} + \frac{\partial^3 w}{\partial x^2 \partial y} - \frac{\partial^2 u}{R_x \partial x \partial y} + \frac{\partial^2 \psi_y}{\partial y^2} + \frac{\partial^3 w}{\partial y^3} - \frac{\partial^2 v}{R_y \partial y^2} \right) \right.$$

$$\left. - c \left(T_{1z3} \frac{\partial \phi}{\partial y} + T_{3z3} \left(\frac{\partial^2 \psi_x}{\partial x \partial y} + \frac{\partial^2 \psi_y}{\partial y^2} \right) + T_{4z3} \left(\frac{\partial^2 \psi_x}{\partial x \partial y} + \frac{\partial^3 w}{\partial x^2 \partial y} - \frac{\partial^2 u}{R_x \partial x \partial y} + \frac{\partial^2 \psi_y}{\partial y^2} + \frac{\partial^3 w}{\partial y^3} - \frac{\partial^2 v}{R_y \partial y^2} \right) \right) \right)$$

$$- \left(T_5 \frac{\partial \phi}{\partial y} + T_7 \left(\frac{\partial^2 \psi_x}{\partial x \partial y} + \frac{\partial^2 \psi_y}{\partial y^2} \right) + T_8 \left(\frac{\partial^2 \psi_x}{\partial x \partial y} + \frac{\partial^3 w}{\partial x^2 \partial y} - \frac{\partial^2 u}{R_x \partial x \partial y} + \frac{\partial^2 \psi_y}{\partial y^2} + \frac{\partial^3 w}{\partial y^3} - \frac{\partial^2 v}{R_y \partial y^2} \right) \right)$$

$$- \beta \left(T_{5z2} \frac{\partial \phi}{\partial y} + T_{7z2} \left(\frac{\partial^2 \psi_x}{\partial x \partial y} + \frac{\partial^2 \psi_y}{\partial y^2} \right) + T_{8z2} \left(\frac{\partial^2 \psi_x}{\partial x \partial y} + \frac{\partial^3 w}{\partial x^2 \partial y} - \frac{\partial^2 u}{R_x \partial x \partial y} + \frac{\partial^2 \psi_y}{\partial y^2} + \frac{\partial^3 w}{\partial y^3} - \frac{\partial^2 v}{R_y \partial y^2} \right) \right)$$

$$= \left(I_1 + \frac{I_2}{R_y} - c I_3 - c \frac{I_4}{R_y} \right) \frac{\partial^2 v}{\partial t^2} + \left(I_2 - 2c I_4 + c^2 I_6 \right) \frac{\partial^2 \psi_y}{\partial t^2} + \left(-c I_4 + c^2 I_6 \right) \frac{\partial^3 w}{\partial y \partial t^2}$$

$$(22.d)$$

$$\delta w : ag_1 \frac{\partial u}{\partial x} + ag_2 \frac{\partial^3 u}{\partial x^3} + ag_3 \frac{\partial^3 u}{\partial x \partial y^2} + ag_4 \frac{\partial v}{\partial y} + ag_5 \frac{\partial^3 v}{\partial x^2 \partial y} + ag_6 \frac{\partial^3 v}{\partial y^3} + ag_7 \frac{\partial \psi_x}{\partial x} + ag_8 \frac{\partial^3 \psi_x}{\partial x^3}$$

$$+ ag_9 \frac{\partial^3 \psi_x}{\partial x^2 \partial y} + ag_{10} \frac{\partial \psi_y}{\partial y} + ag_{11} \frac{\partial^3 \psi_y}{\partial y^3} + ag_{12} \frac{\partial^3 \psi_y}{\partial x^2 \partial y} + ag_{13} \frac{\partial^4 w}{\partial x^4} + ag_{14} \frac{\partial^4 w}{\partial y^4}$$

$$+ ag_{15} \frac{\partial^4 w}{\partial x^2 \partial y^2} + ag_{16} \frac{\partial^2 w}{\partial x^2} + ag_{17} \frac{\partial^2 w}{\partial y^2} + ag_{18} w + T_5 \frac{\partial^2 \phi}{\partial x^2} + T_7 \left(\frac{\partial^3 \psi_x}{\partial x^3} + \frac{\partial^3 \psi_y}{\partial x^2 \partial y} \right)$$

$$+ T_8 \left(\frac{\partial^3 \psi_x}{\partial x^3} + \frac{\partial^4 w}{\partial x^4} - \frac{\partial^3 u}{R_x \partial x^3} + \frac{\partial^3 \psi_y}{\partial x^2 \partial y} + \frac{\partial^4 w}{\partial x^2 \partial y^2} - \frac{\partial^3 v}{R_y \partial x^2 \partial y} \right) - \beta \left(T_{5z2} \frac{\partial^2 \phi}{\partial x^2} + T_{7z2} \left(\frac{\partial^3 \psi_x}{\partial x^3} + \frac{\partial^3 \psi_y}{\partial x^2 \partial y} \right) \right.$$

$$+ T_{8z2} \left(\frac{\partial^3 \psi_x}{\partial x^3} + \frac{\partial^4 w}{\partial x^4} - \frac{\partial^3 u}{R_x \partial x^3} + \frac{\partial^3 \psi_y}{\partial x^2 \partial y} + \frac{\partial^4 w}{\partial x^2 \partial y^2} - \frac{\partial^3 v}{R_y \partial x^2 \partial y} \right) \right) + T_5 \frac{\partial^2 \phi}{\partial y^2}$$

$$+ T_7 \left(\frac{\partial^3 \psi_x}{\partial x \partial y^2} + \frac{\partial^3 \psi_y}{\partial y^3} \right) + T_8 \left(\frac{\partial^3 \psi_y}{\partial y^3} + \frac{\partial^4 w}{\partial y^4} - \frac{\partial^3 v}{R_y \partial y^3} + \frac{\partial^3 \psi_x}{\partial x \partial y^2} + \frac{\partial^4 w}{\partial x^2 \partial y^2} - \frac{\partial^3 u}{R_x \partial x \partial y^2} \right) - \beta \left(T_{5z2} \frac{\partial^2 \phi}{\partial y^2} \right.$$

$$+ T_{7z2} \left(\frac{\partial^3 \psi_x}{\partial x \partial y^2} + \frac{\partial^3 \psi_y}{\partial y^3} \right) + T_{8z2} \left(\frac{\partial^3 \psi_y}{\partial y^3} + \frac{\partial^4 w}{\partial y^4} - \frac{\partial^3 v}{R_y \partial y^3} + \frac{\partial^3 \psi_x}{\partial x \partial y^2} + \frac{\partial^4 w}{\partial x^2 \partial y^2} - \frac{\partial^3 u}{R_x \partial x \partial y^2} \right) \right)$$

$$+ c \left(T_{1z3} \left(\frac{\partial^2 \phi}{\partial x^2} + \frac{\partial^2 \phi}{\partial y^2} \right) + T_{3z3} \left(\frac{\partial^3 \psi_x}{\partial x^3} + \frac{\partial^3 \psi_y}{\partial x^2 \partial y} + \frac{\partial^3 \psi_x}{\partial x \partial y^2} + \frac{\partial^3 \psi_y}{\partial y^3} \right) + T_{4z3} \left(\frac{\partial^3 \psi_x}{\partial x^3} + \frac{\partial^4 w}{\partial x^4} - \frac{\partial^3 u}{R_x \partial x^3} \right. \right.$$

$$+ \frac{\partial^3 \psi_y}{\partial x^2 \partial y} + \frac{\partial^4 w}{\partial x^2 \partial y^2} - \frac{\partial^3 v}{R_y \partial x^2 \partial y} \frac{\partial^3 \psi_y}{\partial y^3} + \frac{\partial^4 w}{\partial y^4} - \frac{\partial^3 v}{R_y \partial y^3} + \frac{\partial^3 \psi_x}{\partial x \partial y^2} + \frac{\partial^4 w}{\partial x^2 \partial y^2} - \frac{\partial^3 u}{R_x \partial x \partial y^2} \right) \right)$$

$$- \frac{T_2}{R_x} \left(\left(\frac{\partial u}{\partial x} + \frac{w}{R_x} \right) + \left(\frac{\partial v}{\partial y} + \frac{w}{R_y} \right) \right) - \frac{T_2}{R_y} \left(\left(\frac{\partial u}{\partial x} + \frac{w}{R_x} \right) + \left(\frac{\partial v}{\partial y} + \frac{w}{R_y} \right) \right) + \Delta P$$

$$= I_0 \frac{\partial^2 w}{\partial t^2} - c \left[\left(I_3 + \frac{I_4}{R_x} \right) \left(\frac{\partial^3 u}{\partial x \partial t^2} \right) + \left(I_3 + \frac{I_4}{R_y} \right) \left(\frac{\partial^3 v}{\partial y \partial t^2} \right) + \left(I_4 - cI_6 \right) \left(\frac{\partial^3 \psi_x}{\partial x \partial t^2} \right) \right.$$

$$+ \left(I_4 - cI_6 \right) \left(\frac{\partial^3 \psi_y}{\partial y \partial t^2} \right) - cI_6 \left(\frac{\partial^4 w}{\partial x^2 \partial t^2} + \frac{\partial^4 w}{\partial y^2 \partial t^2} \right) \right] \tag{22.e}$$

The constant quantities in Eq. (22), have been defined in "Appendix A".
The mechanical boundary conditions can be expressed as
Simply supported boundary conditions (S)

$$\text{at} \quad x = 0, a$$
$$u = 0, v = 0, \psi_y = 0, M_{xx} - cP_{xx} = 0, w = 0, P_{xx} = 0 \tag{23.a}$$

$$\text{at} \quad y = 0, b$$
$$u = 0, v = 0, \psi_x = 0, M_{yy} - cP_{yy} = 0, w = 0, P_{yy} = 0 \tag{23.b}$$

Clamped boundary conditions (C)

$$\text{at} \quad x = 0, a$$
$$u = 0, v = 0, \psi_x = 0, \psi_y = 0, w = 0, \frac{\partial w}{\partial x} = 0 \tag{24.a}$$

$$\text{at} \quad y = 0, b$$
$$u = 0, v = 0, \psi_x = 0, \psi_y = 0, w = 0, \frac{\partial w}{\partial x} = 0 \tag{24.b}$$

The variables have to satisfy Maxwell's equation (Farsangi et al. [69])

$$\int_{-h-h_p}^{-h} \vec{\nabla} \cdot \vec{D} dz + \int_{h}^{h+h_p} \vec{\nabla} \cdot \vec{D} dz = 0 \tag{25}$$

Substituting Eq. (3) and (9), into Eq. (25) yields

$$
\begin{aligned}
&\delta\phi S_1 \left(\frac{\partial \psi_x}{\partial x} + \frac{\partial^2 w}{\partial x^2} - \frac{\partial u}{R_x \partial x} + \frac{\partial \psi_y}{\partial y} + \frac{\partial^2 w}{\partial y^2} - \frac{\partial v}{R_y \partial y} \right) - S_2 \left(\frac{\partial^2 \phi}{\partial x^2} + \frac{\partial^2 \phi}{\partial y^2} \right) \\
&- S_6 \left(\frac{u}{\partial x^3} + \frac{\partial^2 w}{R_x \partial x^2} + \frac{\partial^3 v}{\partial x^2 \partial y} + \frac{\partial^2 w}{R_y \partial x^2} + \frac{\partial^3 u}{\partial x \partial y^2} + \frac{\partial^2 w}{R_x \partial y^2} + \frac{\partial^3 v}{\partial y^3} + \frac{\partial^2 w}{R_y \partial y^2} \right) \\
&+ S_7 \left(\frac{\partial^3 \psi_x}{\partial x^3} + \frac{\partial^3 \psi_y}{\partial x^2 \partial y} + \frac{\partial^3 \psi_x}{\partial x \partial y^2} + \frac{\partial^3 \psi_y}{\partial y^3} \right) + S_8 \left(\frac{\partial^3 \psi_x}{\partial x^3} + \frac{\partial^4 w}{\partial x^4} - \frac{\partial^3 u}{R_x \partial x^3} + \frac{\partial^3 \psi_y}{\partial x^2 \partial y} \right. \\
&+ \frac{\partial^4 w}{\partial x^2 \partial y^2} - \frac{\partial^3 v}{R_y \partial x^2 \partial y} + \frac{\partial^3 \psi_x}{\partial x \partial y^2} + \frac{\partial^4 w}{\partial x^2 \partial y^2} - \frac{\partial^3 u}{R_x \partial x \partial y^2} + \frac{\partial^3 \psi_y}{\partial y^3} + \frac{\partial^4 w}{\partial y^4} - \left. \frac{\partial^3 v}{R_y \partial y^3} \right) \\
&+ S_3 \left(\frac{\partial \psi_x}{\partial x} + \frac{\partial \psi_y}{\partial y} \right) - S_4 \left(\frac{\partial \psi_x}{\partial x} + \frac{\partial^2 w}{\partial x^2} - \frac{\partial u}{R_x \partial x} + \frac{\partial \psi_y}{\partial y} + \frac{\partial^2 w}{\partial y^2} - \frac{\partial v}{R_y \partial y} \right) - S_5 \phi = 0
\end{aligned}
\tag{26}
$$

The electrical boundary conditions at $x = 0, a, \; y = \pm \frac{b}{2}$ are:

$$
\phi(0, y, t) = \phi(a, y, t) = 0 \tag{27}
$$

and

$$
\int_{-h-h_p}^{-h} D_y(x, y, z, t) dz + \int_{h+h_p}^{h} D_y(x, y, z, t) dz = 0 \tag{28}
$$

In "Appendix B", the definitions of constant quantities in Eq. (26) have been presented.

3 Solution technique

The Galerkin method is used to discretize the partial differential equations into ordinary equations. The modal expansions are assumed to approximate the aeroelastic stability analysis of a doubly curved panel made of FG porous as follows. (Fung [75])

$$
\begin{aligned}
u(x, y, t) &= \boldsymbol{\Phi}_u^T \boldsymbol{q}_u, \quad v(x, y, t) = \boldsymbol{\Phi}_v^T \boldsymbol{q}_v, \quad \psi_x(x, y, t) = \boldsymbol{\Phi}_{\psi_x}^T \boldsymbol{q}_{\psi_x}, \\
\psi_y(x, y, t) &= \boldsymbol{\Phi}_{\psi_y}^T \boldsymbol{q}_{\psi_y}, \quad w(x, y, t) = \boldsymbol{\Phi}_w^T \boldsymbol{q}_w, \quad \phi(x, y, t) = \boldsymbol{\Phi}_\phi^T \boldsymbol{q}_\phi
\end{aligned}
\tag{29}
$$

where $\boldsymbol{q}_u, \; \boldsymbol{q}_v, \; \boldsymbol{q}_{\psi_x}, \; \boldsymbol{q}_{\psi_y}, \; \boldsymbol{q}_w$ and $\boldsymbol{q}_\phi$ denote the generalized coordinates; $\boldsymbol{\Phi}_u, \; \boldsymbol{\Phi}_v, \; \boldsymbol{\Phi}_{\psi_x}, \; \boldsymbol{\Phi}_{\psi_y}, \; \boldsymbol{\Phi}_w$ and $\boldsymbol{\Phi}_\phi$ expressed the unknown displacements that satisfy boundary conditions. The unknown displacements $(u, v, \psi_x, \psi_y, w, \phi)$ can be represented as

$$
u(x, y, t) = \boldsymbol{\Phi}_u^T \boldsymbol{q}_u = \sum_{n=1}^{n'} \sum_{m=1}^{m'} q_{umn}(t) \varphi_{um}(x) \psi_{un}(y)
$$

$$
v(x, y, t) = \boldsymbol{\Phi}_v^T \boldsymbol{q}_v = \sum_{n=1}^{n'} \sum_{m=1}^{m'} q_{vmn}(t) \varphi_{vm}(x) \psi_{vn}(y)
$$

$$
\psi_x(x, y, t) = \boldsymbol{\Phi}_{\psi_x}^T \boldsymbol{q}_{\psi_x} = \sum_{n=1}^{n'} \sum_{m=1}^{m'} q_{xmn}(t) \varphi_{xm}(x) \psi_{xn}(y)
$$

$$
\psi_y(x, y, t) = \boldsymbol{\Phi}_{\psi_y}^T \boldsymbol{q}_{\psi_y} = \sum_{n=1}^{n'} \sum_{m=1}^{m'} q_{ymn}(t) \varphi_{ym}(x) \psi_{yn}(y)
$$

$$
w(x, y, t) = \boldsymbol{\Phi}_w^T \boldsymbol{q}_w = \sum_{n=1}^{n'} \sum_{m=1}^{m'} q_{wmn}(t) \varphi_{wm}(x) \psi_{wn}(y)
$$

$$\phi(x, y, t) = \boldsymbol{\Phi}_\phi^T \boldsymbol{q}_\phi = \sum_{n=1}^{n'} \sum_{m=1}^{m'} q_{\phi mn}(t) \varphi_{\phi m}(x) \psi_{\phi n}(y) \tag{30}$$

where m' and n' are the truncation of the Galerkin expansion (or the number of modes). It is shown in Table. 2 that Eq. (30) converges in the sixth mode. So,

$$m' = n' = 6 \tag{31}$$

The unknown displacements that satisfy appropriate simply supported (S) and clamped (C) boundary conditions can be written as

Simply supported (S):

$$\varphi_{rs}(x, y) = \sin\left(r\frac{\pi x}{L}\right) \sin\left(s\frac{\pi y}{L}\right) \tag{32}$$

Clamped (C):

$$\begin{aligned}
\varphi_{rs}(x, y) = {} & (\cosh(k_i x) - \cos(k_i x)) \\
& - D_i(\sinh(k_i x) - \sin(k_i x))(\cosh(k_i y) - \cos(k_i y)) \\
& - D_i(\sinh(k_i y) - \sin(k_i y))
\end{aligned} \tag{33}$$

where

$$D_i = \frac{\sinh(k_i) - \sin(k_i)}{\cosh(k_i) - \cos(k_i)}$$

$$k_1 = 4.7300, \ k_2 = 7.8532, \ k_3 = 10.9956, \ k_4 = 14.1316,$$

$$k_5 = 17.2887, \quad i > 5 \Rightarrow k_i = (2i + 1)\frac{\pi}{2}$$

The Galerkin method is used to discretize form of governing equations which can be given as

$$M\ddot{\boldsymbol{q}}(t) + C\dot{\boldsymbol{q}}(t) + K_e\boldsymbol{q}(t) = 0 \tag{34}$$

In Eq. (34), the overall vector of generalized coordinates is expressed by $\boldsymbol{q} = \left[\boldsymbol{q}_u^T \ \boldsymbol{q}_v^T \ \boldsymbol{q}_{\psi_x}^T \ \boldsymbol{q}_{\psi_y}^T \ \boldsymbol{q}_w^T \ \boldsymbol{q}_\phi^T\right]^T$. Furthermore, K_e, M and C represent the stiffness, mass and damping matrices, respectively. So, the stiffness matrix can be represented as

$$\begin{bmatrix}
\boldsymbol{K}_{11} & \boldsymbol{K}_{12} & \boldsymbol{K}_{13} & \boldsymbol{K}_{14} & \boldsymbol{K}_{15} & \boldsymbol{K}_{16} \\
\boldsymbol{K}_{21} & \boldsymbol{K}_{22} & \boldsymbol{K}_{23} & \boldsymbol{K}_{24} & \boldsymbol{K}_{25} & \boldsymbol{K}_{26} \\
\boldsymbol{K}_{31} & \boldsymbol{K}_{32} & \boldsymbol{K}_{33} & \boldsymbol{K}_{34} & \boldsymbol{K}_{35} & \boldsymbol{K}_{36} \\
\boldsymbol{K}_{41} & \boldsymbol{K}_{42} & \boldsymbol{K}_{43} & \boldsymbol{K}_{44} & \boldsymbol{K}_{45} & \boldsymbol{K}_{46} \\
\boldsymbol{K}_{51} & \boldsymbol{K}_{52} & \boldsymbol{K}_{53} & \boldsymbol{K}_{54} & \boldsymbol{K}_{55} & \boldsymbol{K}_{56} \\
\boldsymbol{K}_{61} & \boldsymbol{K}_{62} & \boldsymbol{K}_{63} & \boldsymbol{K}_{64} & \boldsymbol{K}_{65} & \boldsymbol{K}_{66}
\end{bmatrix}
\begin{Bmatrix}
\boldsymbol{q}_u \\
\boldsymbol{q}_v \\
\boldsymbol{q}_{\psi_x} \\
\boldsymbol{q}_{\psi_x} \\
\boldsymbol{q}_w \\
\boldsymbol{q}_\phi
\end{Bmatrix} = 0 \tag{35}$$

The above equation can be rewritten as

$$\begin{aligned}
\overline{\boldsymbol{K}}_{11}\boldsymbol{q} + \overline{\boldsymbol{K}}_{12}\boldsymbol{q}_\phi = 0 \\
\overline{\boldsymbol{K}}_{21}\boldsymbol{q} + \overline{\boldsymbol{K}}_{66}\boldsymbol{q}_\phi = 0
\end{aligned} \tag{36}$$

$$\overline{\boldsymbol{K}}_{11} = \begin{bmatrix}
\boldsymbol{K}_{11} & \boldsymbol{K}_{12} & \boldsymbol{K}_{13} & \boldsymbol{K}_{14} & \boldsymbol{K}_{15} \\
\boldsymbol{K}_{21} & \boldsymbol{K}_{22} & \boldsymbol{K}_{23} & \boldsymbol{K}_{24} & \boldsymbol{K}_{25} \\
\boldsymbol{K}_{31} & \boldsymbol{K}_{32} & \boldsymbol{K}_{33} & \boldsymbol{K}_{34} & \boldsymbol{K}_{35} \\
\boldsymbol{K}_{41} & \boldsymbol{K}_{42} & \boldsymbol{K}_{43} & \boldsymbol{K}_{44} & \boldsymbol{K}_{45} \\
\boldsymbol{K}_{51} & \boldsymbol{K}_{52} & \boldsymbol{K}_{53} & \boldsymbol{K}_{54} & \boldsymbol{K}_{55} \\
\boldsymbol{K}_{61} & \boldsymbol{K}_{62} & \boldsymbol{K}_{63} & \boldsymbol{K}_{64} & \boldsymbol{K}_{65}
\end{bmatrix}, \boldsymbol{q} = \left\{\boldsymbol{q}_u \ \boldsymbol{q}_v \ \boldsymbol{q}_{\psi_x} \ \boldsymbol{q}_{\psi_y} \ \boldsymbol{q}_w\right\}^T \tag{37a}$$

$$\overline{\boldsymbol{K}}_{12} = [\boldsymbol{K}_{16} \ \boldsymbol{K}_{26} \ \boldsymbol{K}_{36} \ \boldsymbol{K}_{46} \ \boldsymbol{K}_{56}]^T \tag{37b}$$

$$\overline{\boldsymbol{K}}_{21} = [\boldsymbol{K}_{61} \ \boldsymbol{K}_{62} \ \boldsymbol{K}_{63} \ \boldsymbol{K}_{64} \ \boldsymbol{K}_{65}] \tag{37c}$$

where

$$\boldsymbol{K_e} = \overline{\boldsymbol{K}}_{11} - \overline{\boldsymbol{K}}_{12}\overline{\boldsymbol{K}}_{66}^{-1}\overline{\boldsymbol{K}}_{21} \tag{38}$$

The state vector $\boldsymbol{Z}(t) = \{\boldsymbol{q}(t), \dot{\boldsymbol{q}}(t)\}^T$ is defined and the Eq. (34) can be rewritten as

$$\dot{\boldsymbol{Z}}(t) = \boldsymbol{D}\boldsymbol{Z}(t), \tag{39}$$

where

$$\boldsymbol{D} = \begin{bmatrix} 0 & \boldsymbol{I} \\ -\boldsymbol{M}^{-1}\boldsymbol{K_e} & -\boldsymbol{M}^{-1}\boldsymbol{C} \end{bmatrix}, \tag{40}$$

$\boldsymbol{I}$ is the identity matrix.

Finally, substituting the state vector $\boldsymbol{Z}(t) = \overline{\boldsymbol{Z}}e^{(\omega t)}$ into Eq. (39) yields

$$(\boldsymbol{D} - i\omega\boldsymbol{I})\overline{\boldsymbol{Z}} = 0. \tag{41}$$

From Eq. (41), the eigenvalues ω's are obtained which are generally complex quantities and written as a form, $\omega = \omega_R + i\omega_I$. So ω_I represents the natural frequency of the system and ω_R is a real part. Dynamic instability occurs when the real part of the eigenvalue sign becomes positive. The aerodynamic pressure associated with this signal change is represented by the critical flutter aerodynamic pressure, λ_{cr}. This phenomenon is caused by the merging of two modes of torsion and bending, which is known as the flutter frequency, ω_{cr} (Saidi et al. [30]).

4 Numerical results

The dimensionless parameters can be defined as

$$\Omega = \omega\left(\sqrt{\frac{D_m}{2\rho_t h a^4}}\right), D_m = \frac{2E_t h^3}{3(1 - v_t^2)} \tag{42}$$

To evaluate the accuracy of the results obtained for vibration and dynamic instability analyses of FG Porous doubly curved Panels, a comparison has been made with some published results (e.g. [9, 21, 31, 72–74]). In Table 1, a comparison between the obtained results and those reported in the references (Matsunaga. [72], Chorfi and Houmat [9]) for FGM curved shells under simply supported boundary conditions has been made. For this validation, the material of the shell is considered according to the mentioned references, (Al/Al$_2$O$_3$). The thickness of the piezoelectric layers and porosity coefficient is considered $(h_p = 10^{-10}\text{m})$ and $(e = 10^{-10}$m$)$ in order to obtain a curved shell similar to the mentioned references with a very good approximation. As it can be found from Table 1, good correlation between the results of the present analysis and the results obtained in the previous references can be seen. Also, the flutter aerodynamic pressure λ_{cr} and flutter frequency (ω_{cr}) for an isotropic square plate have been compared with the results presented by Prakash and Ganapathi [74] and Akbari et al. [73] in Table 2. It should be mentioned that Akbari et al. [73] used the generalized differential quadrature method (GDQM) and Prakash and Ganapathi [74] used the finite element method (FEM) for flutter analysis.

The non-dimensional frequencies $\overline{\omega} = \omega h\sqrt{\rho_m/E_m}$ of an SCSC and SSSS FG porous plate for power-law indices, porosity distributions, thickness-side ratios, various aspect ratios and porosity parameters have been compared with the results have been provided by Rezaei et al. [21], in Table 3. In Table 4, the flutter frequency ω_{cr} and flutter aerodynamic pressure λ_{cr} of SSSS, CSCS and CCCC porous plate $(b/a = 1, h_p/2h = 0.05$ and $2h/a = 0.1)$ have been compared with the results have been presented by Bahaadini et al. [31]. As can be seen from these tables, there is a good agreement between the presented results and the results of previous research. The material properties of FG porous core and piezoelectric layers are prepared in Tables 5 and 6. Then the flutter boundaries for this system are studied using the Galerkin method. Table 7 shows the influence of different types of porosity coefficients and power-law index on the flutter aerodynamic pressure and flutter frequency. The effects of various piezoelectric layers, radii of principal curvatures of the middle surface (R_x, R_y), FG porous distributions, power-law index, porosity coefficient, doubly curved panel thickness, electrical conditions (open condition and closed condition) and mechanical boundary conditions on the flutter boundaries of FG porous doubly curved panel are studied in Figs. 2, 3, 4,

Table 1 The comparison of the natural frequency, for a FGM (Al/Al$_2$O$_3$) shell $\left(\omega^* = \omega h\sqrt{\frac{\rho}{E}}, , a/h = 10, a/b = 1\right)$

	b/Ry	a/Rx	k	Matsunaga. [72]	Chorfi and Houmat. [9]	Present study
Spherical shell	0.5	0.5	0	0.0751	0.0762	0.07586
			0.5	0.0657	0.0664	0.06602
			1	0.0601	0.0607	0.06052
			4	0.0503	0.0509	0.05061
			10	0.0464	0.0471	0.04676
Cylindrical shell	0	0.5	0	0.0622	0.0629	0.06227
			0.5	0.0535	0.0540	0.05372
			1	0.0485	0.0490	0.04860
			4	0.0413	0.0419	0.04160
			10	0.0390	0.0395	0.03930
Hyperbolic paraboloid shell	-0.5	0.5	0	0.0563	0.0580	0.05661
			0.5	0.0479	0.0493	0.04810
			1	0.0432	0.0445	0.04393
			4	0.0372	0.0385	0.03791
			10	0.0355	0.0368	0.03598
Plate	0	0	0	0.0578	0.0577	0.05777
			0.5	0.0492	0.0490	0.04916
			1	0.0443	0.0442	0.04430
			4	0.0381	0.0383	0.03826
			10	0.0364	0.0366	0.03657

Table 2 The comparison of the flutter aerodynamic pressure λ_{cr} and flutter frequency (ω_{cr}) for an isotropic square plate

		SSSS		CCCC	
		λ_{cr}	ω_{cr}	λ_{cr}	ω_{cr}
Prakash and Ganapathi. [74] (FEM)		511.11	42.90	852.34	65.38
Akbari et al. [73](GDQM)		511.15	43.29	851.27	65.73
Present study	$m' = n' = 7$	511.1881	42.8496	851.3446	65.4805
	$m' = n' = 6$	511.1753	42.8371	851.3283	65.4770
	$m' = n' = 5$	512.9601	43.7523	852.8126	64.6348
	$m' = n' = 4$	503.1282	39.9621	843.7691	59.8216
	$m' = n' = 3$	550.3125	41.1745	890.1642	62.3678
	$m' = n' = 2$	373.7461	36.5123	713.8873	57.4896

Table 3 The comparison of the non-dimensional frequency, $\overline{\omega} = \omega h\sqrt{\rho_m/E_m}, \frac{h}{a} = 0.05, \frac{a}{b} = 1$

Boundary conditions	e		n = 0		n = 0.5		n = 1	
			Even	Uneven	Even	Uneven n	Even	Uneven
SSSS	0	Rezaei et al. [21]	0.029119	0.029119	0.024673	0.024673	0.022237	0.022237
		Present study	0.029108	0.029108	0.024661	0.024661	0.022232	0.022232
	0.2	Rezaei et al. [21]	0.030033	0.029989	0.024558	0.025237	0.021038	0.022473
		Present study	0.030011	0.029971	0.024532	0.025225	0.021022	0.022451
	0.4	Rezaei et al. [21]	0.031371	0.031006	0.024230	0.025896	0.0187173	0.022694
		Present study	0.031342	0.031003	0.024227	0.025882	0.018764	0.022681
CSCS	0	Rezaei et al. [21]	0.042402	0.042402	0.035954	0.035954	0.032414	0.032414
		Present study	0.042401	0.04201	0.035932	0.035932	0.032402	0.032402
	0.2	Rezaei et al. [21]	0.043732	0.043659	0.035796	0.036768	0.030686	0.032754
		Present study	0.043715	0.043647	0.035783	0.036752	0.030675	0.032741
	0.4	Rezaei et al. [21]	0.045681	0.045127	0.035333	0.037719	0.026542	0.033073
		Present study	0.045673	0.045112	0.035321	0.037701	0.026531	0.033061

Table 4 The comparison of flutter aerodynamic pressure and flutter frequency of symmetric porous plate ($e_0 = 0.35$, $2h/a = 0.15$)

Boundary condition	$\frac{h_p}{2h}$	Condition		λ_{cr}	ω_{cr}
CCCC	0	–	Bahaadini et al. [31]	432.730	48.814
			Present study	432.730	48.814
	0.05	Closed	Bahaadini et al. [31]	570.572	49.066
			Present study	570.572	49.066
		Open	Bahaadini et al. [31]	614.08	51.385
			Present study	614.08	51.385
	0.1	Closed	Bahaadini et al. [31]	720.224	49.795
			Present study	720.224	49.795
		Open	Bahaadini et al. [31]	859.860	56.195
			Present study	859.860	56.195
CSCS	0	–	Bahaadini et al. [31]	392.376	43.252
			Present study	392.376	43.252
	0.05	Closed	Bahaadini et al. [31]	521.270	43.456
			Present study	521.270	43.456
		Open	Bahaadini et al. [31]	557.692	45.165
			Present study	557.692	45.165
	0.1	Closed	Bahaadini et al. [31]	665.675	44.147
			Present study	665.675	44.147
		Open	Bahaadini et al. [31]	755.854	47.710
			Present study	755.854	47.710
SSSS	0	–	Bahaadini et al. [31]	349.715	38.601
			Present study	349.715	38.601
	0.05	Closed	Bahaadini et al. [31]	466.580	38.915
			Present study	466.580	38.915
		Open	Bahaadini et al. [31]	496.104	40.290
			Present study	496.104	40.290
	0.1	Closed	Bahaadini et al. [31]	596.875	39.620
			Present study	596.875	39.620
		Open	Bahaadini et al. [31]	651.492	41.865
			Present study	651.492	41.865

Table 5 The material properties of the piezoelectric layer

Property	Piezoelectric layer		
	(PZT-4)	(PZT-5A)	(PZT-5H)
c_{11} (GPa)	132	121	151
c_{12} (GPa)	71	75.4	98
c_{33} (GPa)	115	111	124
c_{13} (GPa)	73	75.2	96
c_{55} (GPa)	26	21.1	26.5
e_{31} $\left(\text{cm}^{-2}\right)$	-4.1	-5.4	-5.1
e_{33} $\left(\text{cm}^{-2}\right)$	14.1	15.8	27
e_{15} $\left(\text{cm}^{-2}\right)$	10.5	12.3	17
Ξ_{11} $\left(\text{nFm}^{-1}\right)$	7.124	8.107	15
Ξ_{33} $\left(\text{nFm}^{-1}\right)$	5.841	7.346	13.27
ρ $\left(\text{kgm}^{-3}\right)$	7500	7700	7400

Table 6 Material properties of FG material

|	E (GPa)	ρ $\left(\text{Kg}/m^3\right)$	v
Al	70	2702	0.3
Al$_2$O$_3$	380	3800	0.3

(a)

(b)
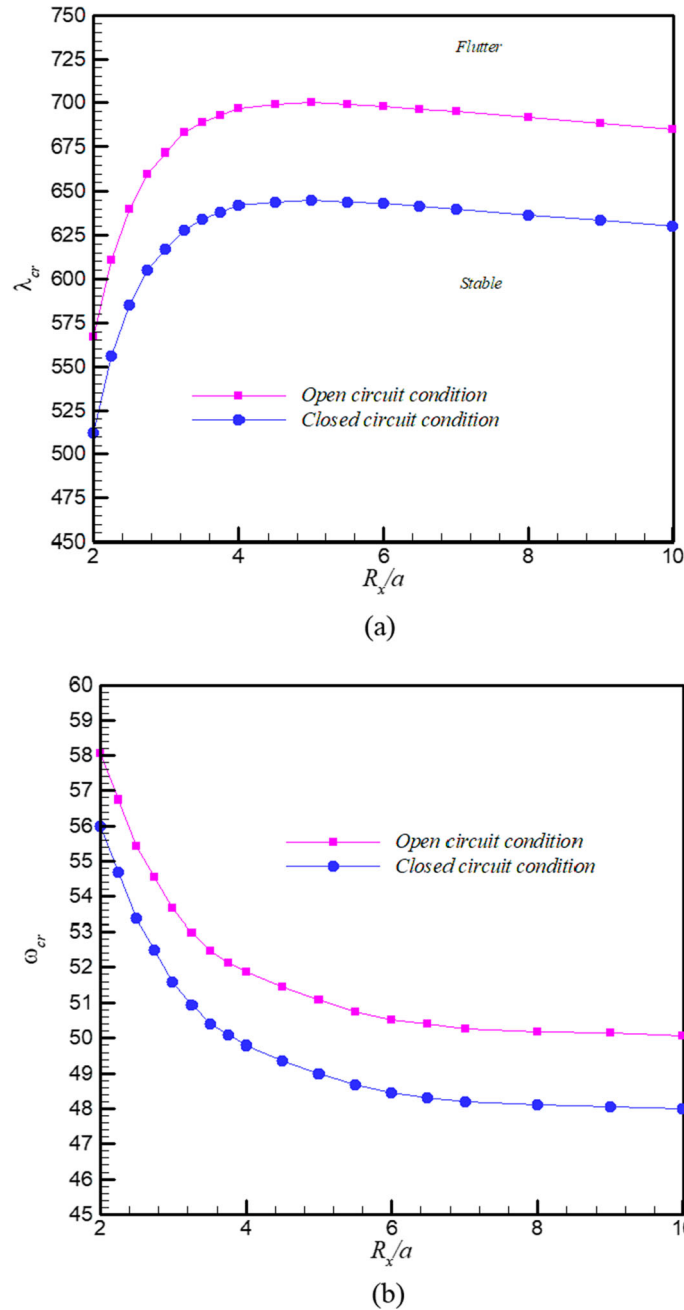
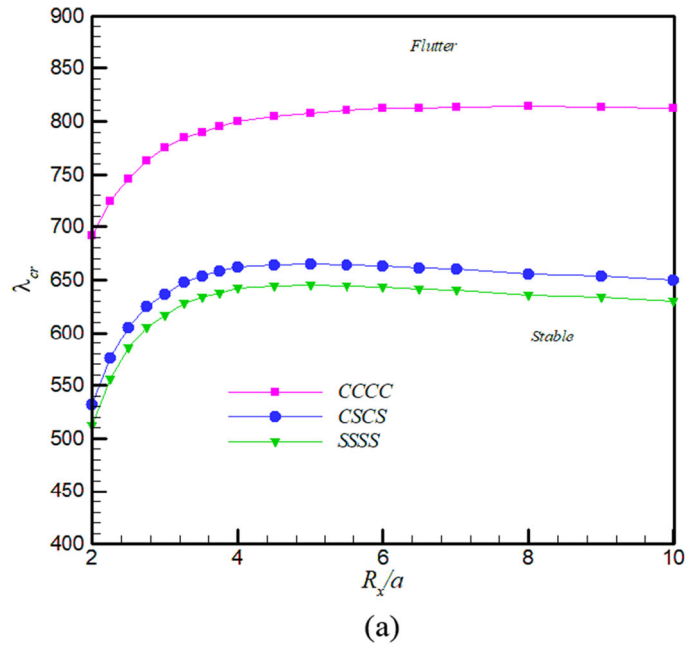**Fig. 2** Flutter boundary versus R_x/a for different circuit conditions for ($PZT-4$, $b/a=1$, $h_p/2h=0.05$, $n=1$, $e=0.1$) **a** critical aerodynamic pressure, **b** critical frequency

5, 6, 7, 8, 9, 10, 11. In Figs. 2, 3, 4, 5, 6, 7, 8, 9, 10, 11. The diagrams show the boundary between dynamic stability and instability. In a stable area, these vibrations are dumped, ie the air acts as a damper, while in an unstable region, the oscillations grow exponentially, leading to a flutter phenomenon.

In these figures, the effects of various piezoelectric layers, radii of principal curvatures of the middle surface (R_x, R_y), FG porous distributions and power-law index on the flutter boundaries of FG porous doubly curved panels are investigated.

In Fig. 2 The influences of open circuit conditions and closed circuit conditions on the flutter boundaries of FG porous doubly curved panels in supersonic flow are performed. It can be seen from Fig. 2 that the open circuit condition predicts a higher stability boundary than the closed circuit condition. The effects of different

(a)

(b)
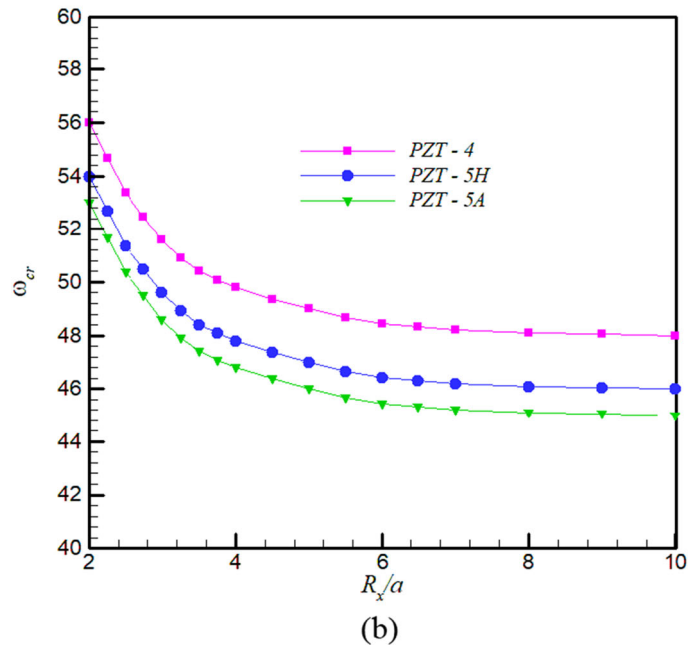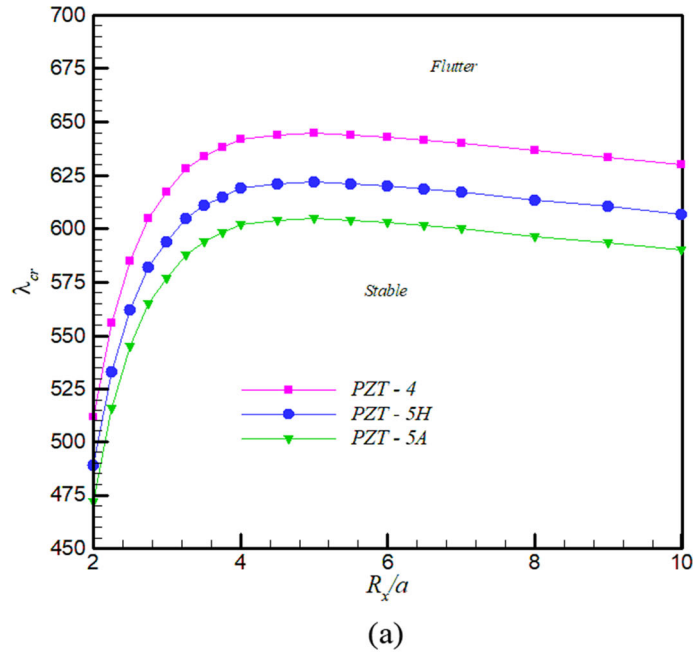
Fig. 3 Flutter boundary versus R_x/a for different Piezoelectric layers for ($b/a = 1$, $h_p/2h = 0.05$, $n = 1$, $e = 0.1$) **a** critical aerodynamic pressure, **b** critical frequency

piezoelectric layers on the flutter boundaries of FG porous doubly curved panels are studied in Fig. 3. From Fig. 3, can be observed that the PZT − 4 predicts the highest flutter boundaries for the FG porous doubly curved panel. In Fig. 4, the effects of mechanical boundary conditions on the flutter boundaries of the system are investigated. It can be seen from Fig. 4 that the clamped boundary conditions predict the highest stability boundaries. It also has the least stability with simply supported boundary conditions. Figure 5 shows the effects of the power-law index on the flutter boundaries. It can be seen from Fig. 5 that increasing the power-law index reduces the stability. Figure 6 shows the influences of porosity coefficient on the flutter boundaries. It can be observed from Fig. 6 that increasing the porosity coefficient reduces the stability. The effects of panel

(a)

(b)
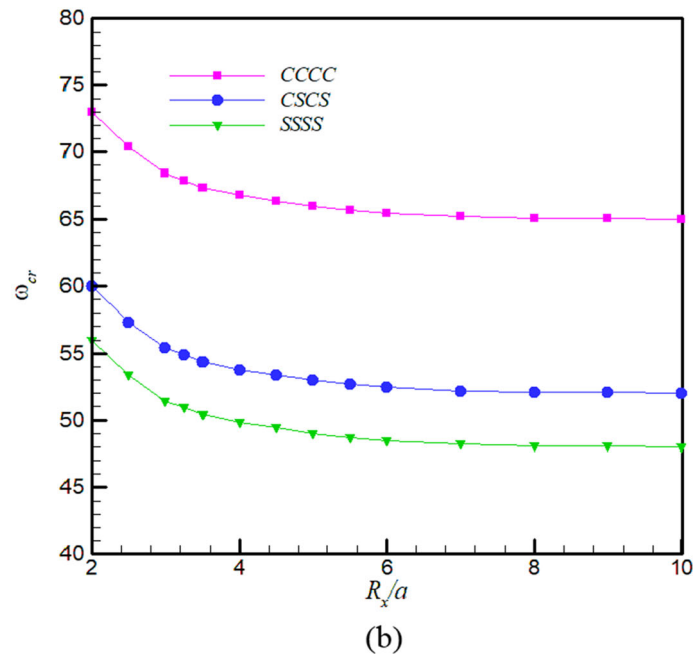
Fig. 4 Flutter boundary versus R_x/a for different mechanical boundary conditions for ($b/a = 1$, $h_p/2h = 0.05$, $n = 1$, $e = 0.1$) **a** critical aerodynamic pressure, **b** critical frequency

dimensions on the flutter boundaries of FG porous doubly curved panels have been investigated in Figs. 7, 8, 9. Figure 7 indicates the variation of flutter boundaries for different aspect ratios. The results show that increasing the aspect ratios reduces the stability boundary. In Fig. 8, the influences of the core panel's thickness on the stability of the system are studied. It can be observed from Fig. 8 that increasing the thickness-length ratios decreases the stability. Figure 9, shows the effects of piezoelectric layer thickness on the flutter boundaries. Examination of the results shows that increasing the thickness of the piezoelectric layer increases the stability of the system. The effects of different FG porous materials on the flutter boundaries of FG porous doubly curved panels are studied in Fig. 10. It is clear from Fig. 10 that the use of V distribution raises the flutter
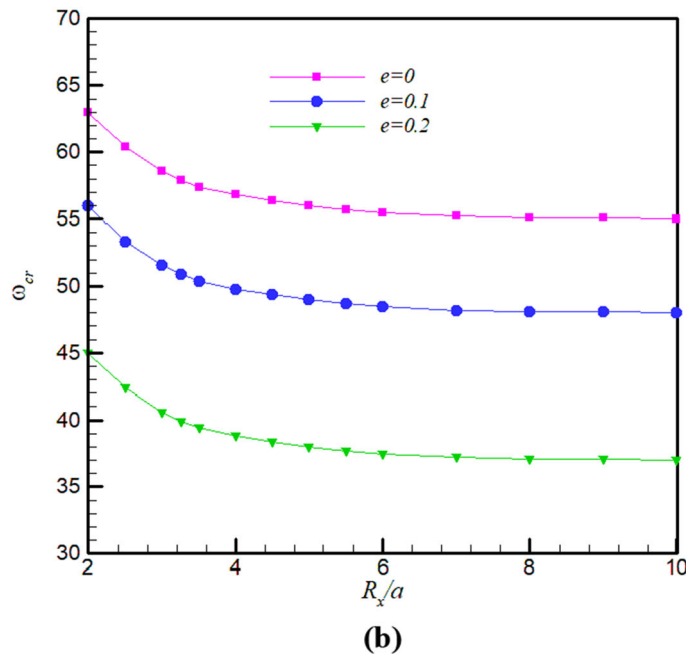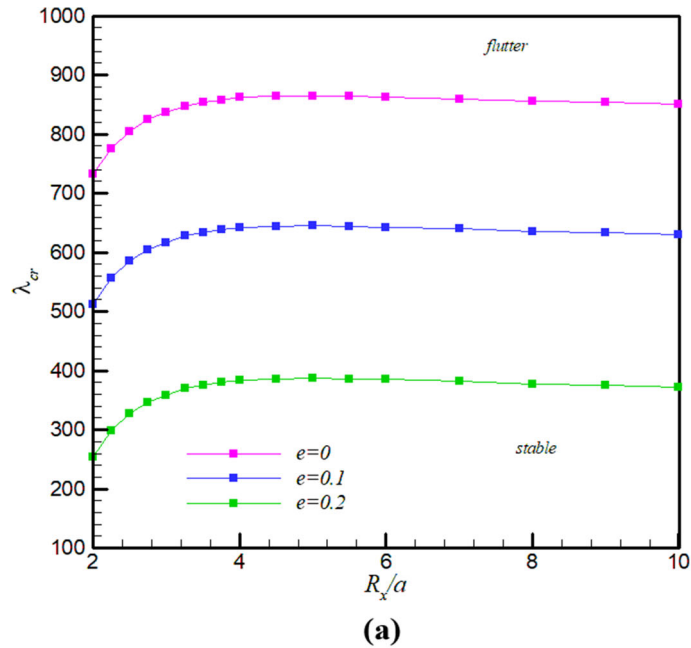
Fig. 5 Flutter boundary versus R_x/a for the different power-law index for $(b/a = 1, \quad h_p/2h = 0.05, \quad e = 0.1)$ **a** critical aerodynamic pressure, **b** critical frequency

boundaries. Figure 11, shows the influences of a different curved panel on the flutter boundaries. A comparison of the curves in Fig. 11 shows that the spherical panel has the highest stability. Figure 10 shows that the stability boundary of the spherical panel is higher than that of the doubly curved panel $\left(R_y = 2R_x\right)$, cylindrical panel, $\left(R_y = -R_x\right)$ and plate.
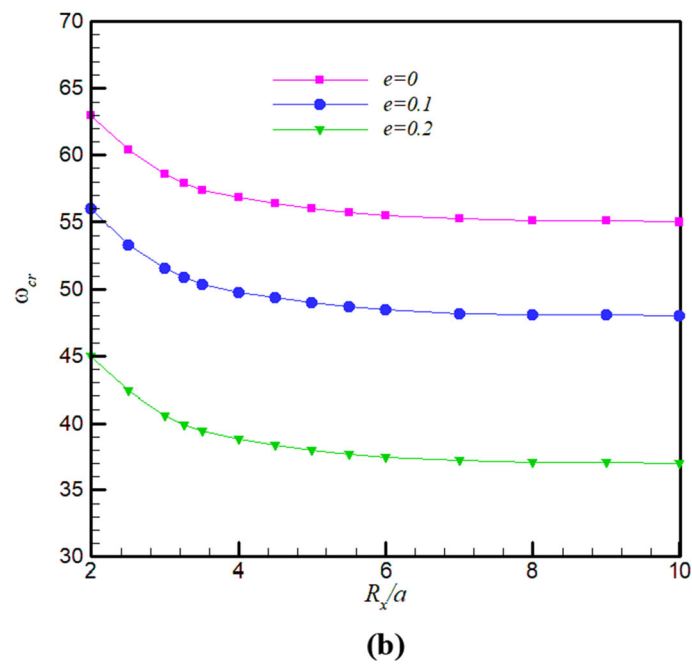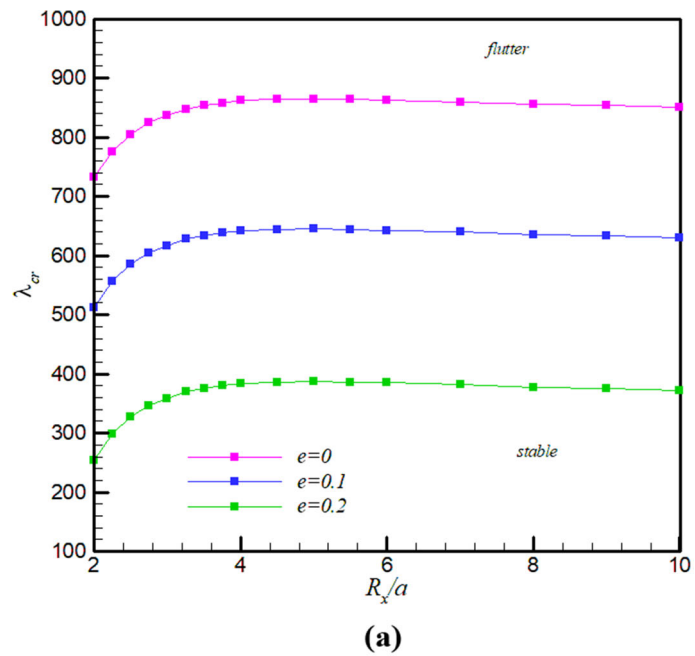
Fig. 6 Flutter boundary versus R_x/a for different porosity for ($b/a = 1$, $h_p/2h = 0.05$, $e = 0.1$) **a** critical aerodynamic pressure, **b** critical frequency
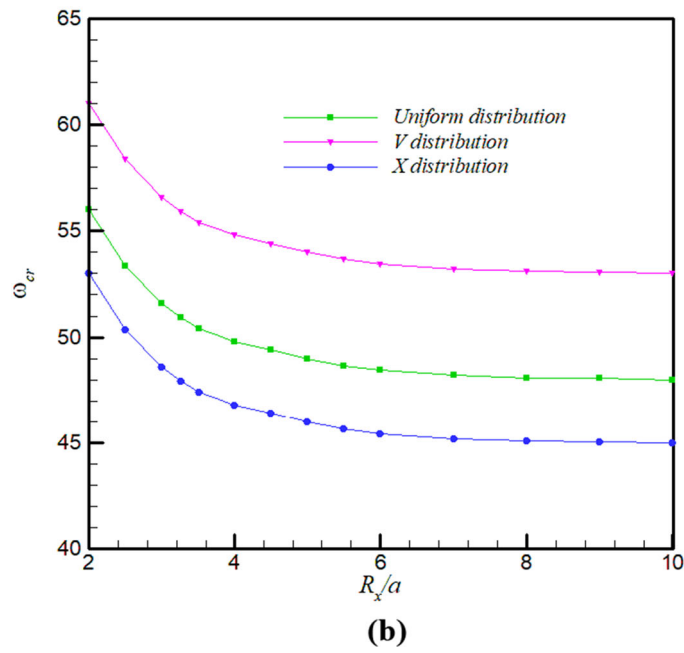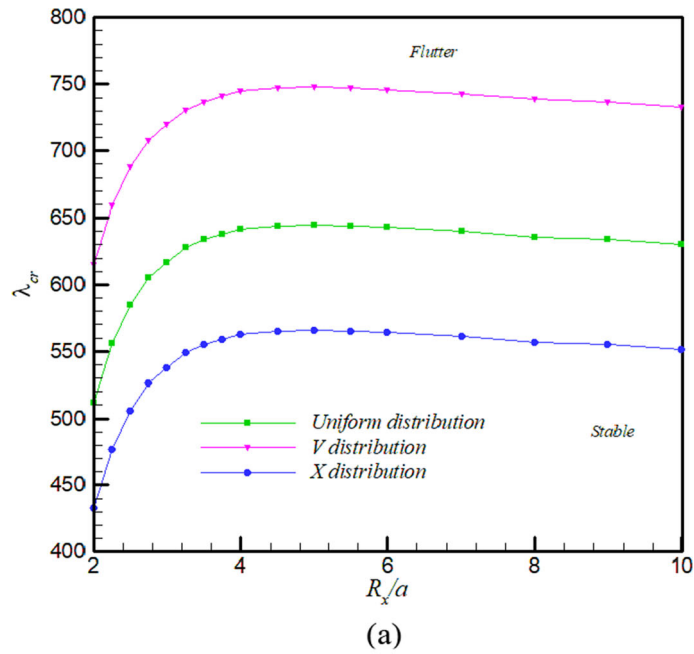
Fig. 7 Flutter boundary versus R_x/a for different FG porous panels for $(h_p/2h = 0.05, \; e = 0.1)$ **a** critical aerodynamic pressure, **b** critical frequency
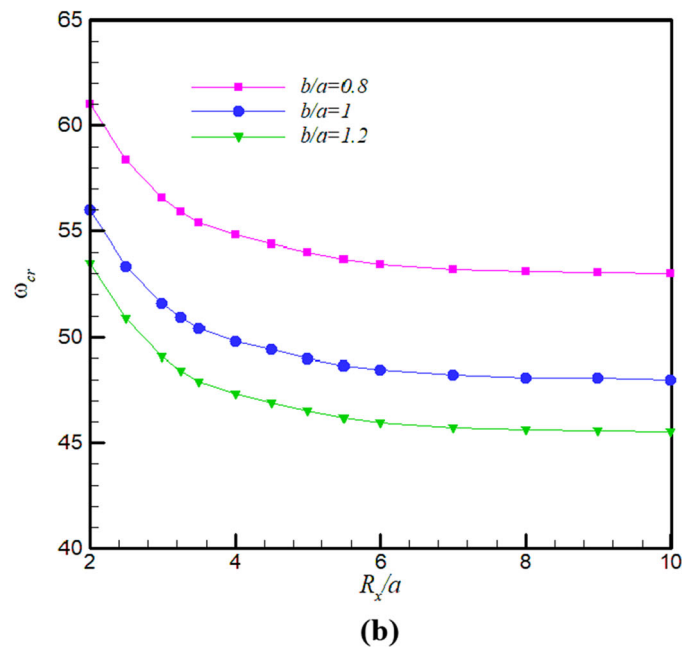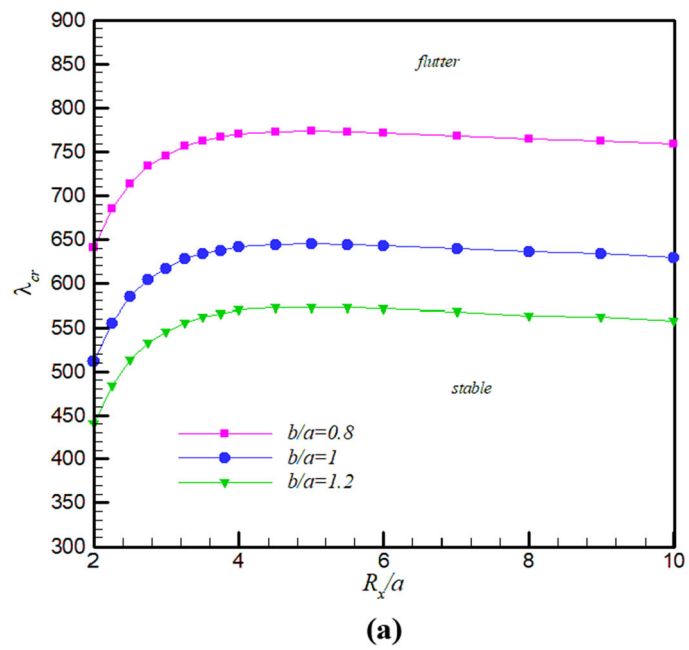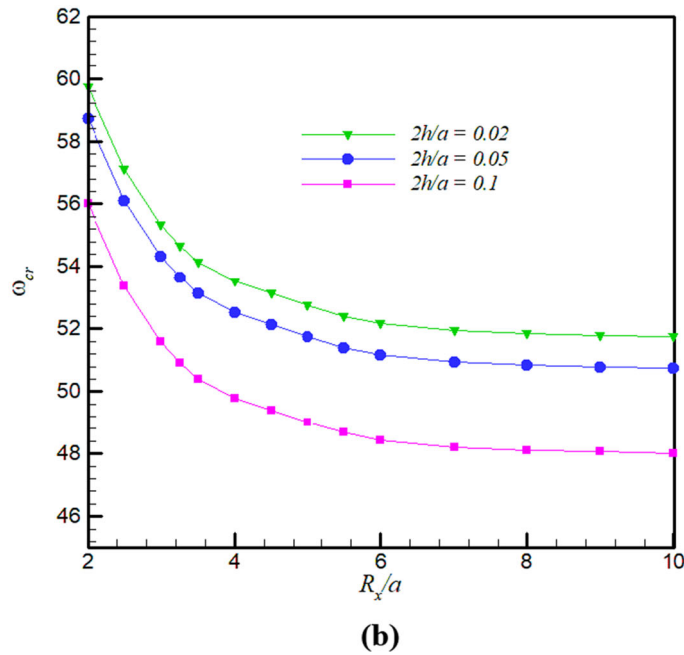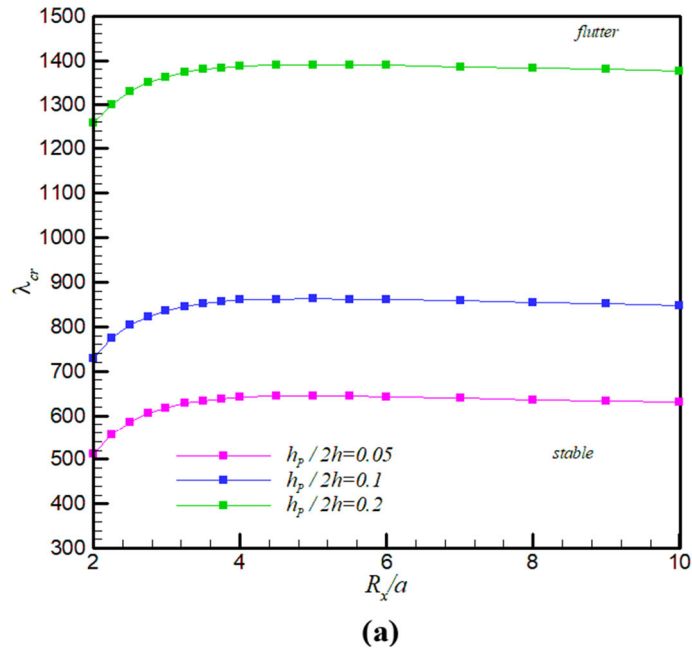
Fig. 8 Flutter boundary versus R_x/a for different (b/a) for $(h_p/2h = 0.05, \ e = 0.1)$ **a** critical aerodynamic pressure, **b** critical frequency
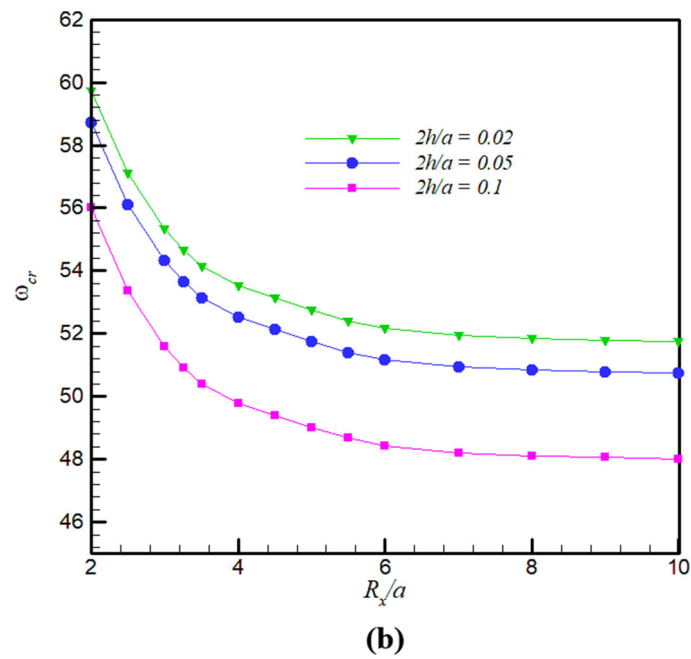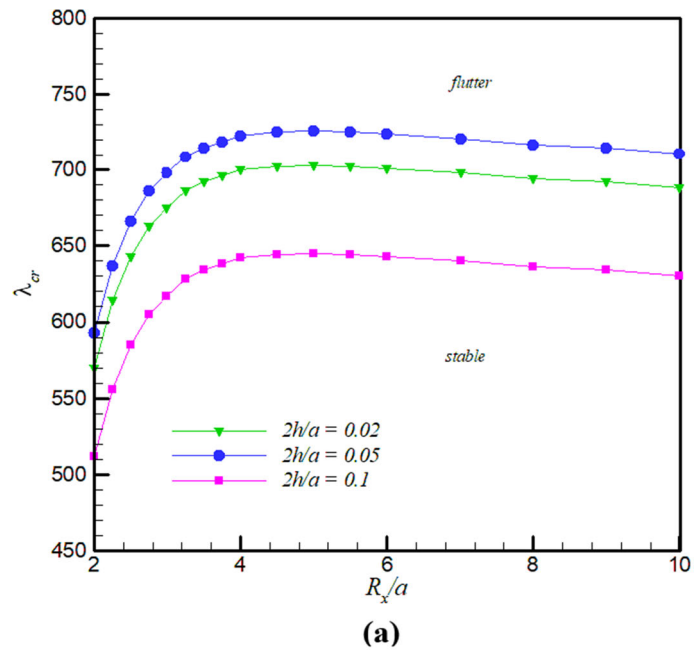
(a)

(b)

Fig. 9 Flutter boundary versus R_x/a for different piezoelectric layer thickness for ($b/a = 1$, $n = 1$, $e = 0.1$) **a** flutter aerodynamic pressure, **b** flutter frequency

(a)

(b)

Fig. 10 Flutter boundary versus R_x/a for different piezoelectric layer thickness for ($b/a = 1, \ n = 1, \ e = 0.1$) **a** flutter aerodynamic pressure, **b** flutter frequency
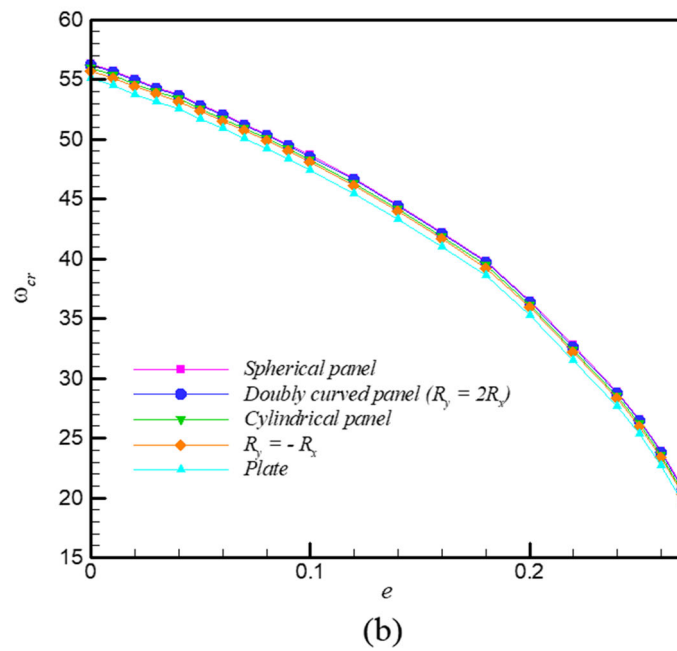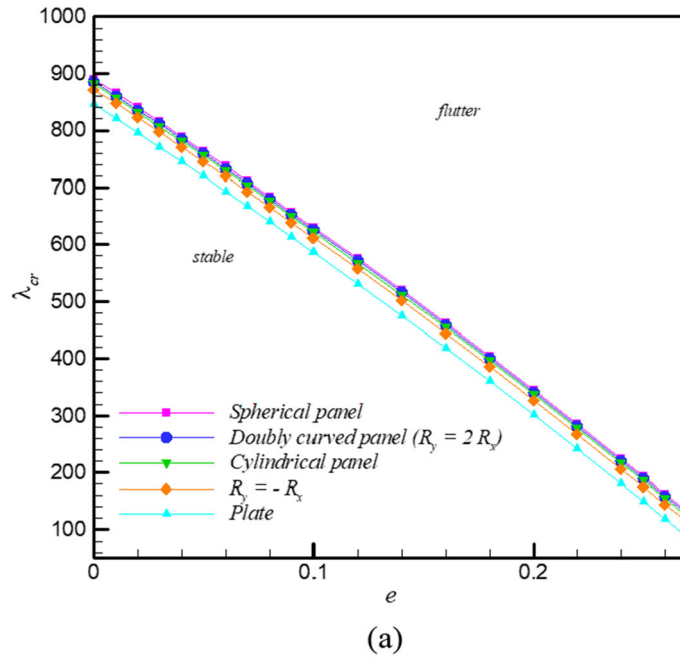
(a)

(b)

Fig. 11 Flutter boundary versus e for a different curved panel for ($b/a = 1$, $h_p/2h = 0.05$, $n = 1$, $R_x/a = 10$) **a** critical aerodynamic pressure, **b** critical frequency

Table 7 The influence of different types of porosity coefficient and power-law index on the flutter aerodynamic pressure and flutter frequency of SSSS FG porous doubly curved panels ($b/a = 1$, $hp/2h = 0.05$ and $2h/a = 0.1$)

	Condition	Aero-elastic parameter	$e = 0$	$e = 0.1$	$e = 0.2$
Spherical panel	Closed	λ_{cr}	890.465	630.212	344.843
		ω_{cr}	55.387	48.072	36.452
	Open	λ_{cr}	943.785	685.124	403.867
		ω_{cr}	56.947	50.0615	40.546
Doubly curved panel ($R_y = 2R_x$)	Closed	λ_{cr}	886.175	626.346	341.912
		ω_{cr}	54.841	47.56	36.115
	Open	λ_{cr}	939.243	682.158	400.011
		ω_{cr}	56.442	49.832	39.151
Cylindrical panel	Closed	λ_{cr}	881.875	622.317	338.134
		ω_{cr}	54.412	47.033	35.971
	Open	λ_{cr}	934.012	677.312	395.883
		ω_{cr}	56.143	49.567	38.911
$R_y = -R_x$	Closed	λ_{cr}	871.965	613.754	330.915
		ω_{cr}	54.143	46.934	35.841
	Open	λ_{cr}	923.233	666.932	387.331
		ω_{cr}	56.021	49.382	38.781
Plate	Closed	λ_{cr}	846.226	591.843	315.872
		ω_{cr}	53.924	46.128	35.447
	Open	λ_{cr}	897.756	645.146	371.688
		ω_{cr}	55.817	49.113	38.142

5 Conclusion

In this study, the flutter boundaries for a doubly curved panel made of FG porous materials surrounded by piezoelectric layers subjected to supersonic flow have been investigated. The governing equations of motion are obtained from Hamilton's principle and Maxwell's equation. In this regard, first-order piston theory and Reddy's third-order shear deformation theory are used. The Galerkin method is used to discretize the equations of motion. Based on the present research, the following results have been obtained:

1. A comparison of the spherical panel, doubly curved panel with $R_y = 2R_x$ and $R_y = -R_x$, cylindrical panel, and plate shows that the spherical panel has the highest and the plate has the lowest stability regions.
2. As the radius to length of the panel increases, the critical flutter aerodynamic pressure increases and the flutter frequency decreases.
3. The open-circuit electrical boundary condition predicts a higher flutter boundary as well as a higher flutter frequency than the closed-circuit electrical boundary condition. Also, the highest and lowest critical flutter aerodynamic pressure and flutter frequency are related to CCCC and SSSS mechanical boundary conditions, respectively.
4. By examining three piezoelectric materials, the PZT-4 type has the highest flutter boundary and flutter frequency, and the PZT-5A type has the lowest critical flutter aerodynamic pressure and flutter frequency. Also, increasing the ratio of piezoelectric layer thickness to panel thickness increases the critical flutter aerodynamic pressure and flutter frequency.
5. The stability of the system decreases by increasing the thickness to length, the width-length ratio, the power law index and the porosity coefficient.
6. Examination of different material distributions shows that V-distribution predicts the highest flutter boundary and flutter frequency.

Appendix A

In Eq. (20), the terms expressing inertia and the resulting forces and moments are expressed as follows:

$$(I_0, I_1, I_2, I_3, I_4, I_6) = \int_{-h-h_p}^{h+h_p} \rho(z)(1, z, z^2, z^3, z^4, z^6)dz \tag{A.1}$$

$$(N_{xx}, N_{xy}, N_{yy}) = \int_{-h-h_p}^{h+h_p} (\sigma_{xx}, \sigma_{xy}, \sigma_{yy})dz$$

$$(M_{xx}, M_{xy}, M_{yy}) = \int_{-h-h_p}^{h+h_p} (\sigma_{xx}, \sigma_{xy}, \sigma_{yy})zdz$$

$$(Q_x, Q_y) = \int_{-h-h_p}^{h+h_p} (\sigma_{xz}, \sigma_{yz})dz$$

$$(S_{xx}, S_{xy}, S_{yy}) = \int_{-h-h_p}^{h+h_p} (\sigma_{xx}, \sigma_{xy}, \sigma_{yy})z^3 dz$$

$$(P_x, P_y) = \int_{-h-h_p}^{h+h_p} (\sigma_{xz}, \sigma_{yz})z^2 dz \tag{A.2}$$

The stiffness coefficients are presented in Eq. (21) as follows:

$$(A_{11}, A_{12}) = \int_{-h}^{-h} (Q_{11}, Q_{12})dz + 2\int_{h}^{h+h_p} (\bar{c}_{11}, \bar{c}_{12})dz$$

$$A_{66} = \int_{-h}^{-h} Q_{66}dz + 2\int_{h}^{h+h_p} (\bar{c}_{11} - \bar{c}_{12})dz$$

$$(B_{11}, B_{12}, B_{66}) = \int_{-h}^{-h} (Q_{11}, Q_{12}, Q_{66})zdz$$

$$(C_{11}, C_{12}, C_{66}) = \int_{-h}^{-h} (Q_{11}, Q_{12}, Q_{66})cz^3 dz$$

$$(D_{11}, D_{12}, D_{66}) = \int_{-h}^{-h} (Q_{11}, Q_{12}, Q_{66})z^2 dz + 2\int_{h}^{h+h_p} (\bar{c}_{11}, \bar{c}_{12}, (\bar{c}_{11} - \bar{c}_{12}))z^2 dz$$

$$(E_{11}, E_{12}) = \int_{-h}^{-h} (Q_{11}, Q_{12})(z^2 - cz^4)dz + 2\int_{h}^{h+h_p} (\bar{c}_{11}, \bar{c}_{12})(z^2 - cz^4)dz$$

$$E_{66} = \int_{-h}^{-h} (Q_{66})(z^2 - cz^4)dz + 2\int_{h}^{h+h_p} (\bar{c}_{11} - \bar{c}_{12})(z^2 - cz^4)dz$$

$$(F_{11}, F_{12}) = \int_{-h}^{-h} (Q_{11}, Q_{12})cz^4 dz + 2 \int_{h}^{h+h_p} (\bar{c}_{11}, \bar{c}_{12})cz^4 dz + \eta_3$$

$$F_{66} = 2 \int_{-h}^{-h} (Q_{66})cz^4 dz + 2 \int_{h}^{h+h_p} (\bar{c}_{11} - \bar{c}_{12})cz^4 dz$$

$$A_{55} = \int_{-h}^{-h} (Q_{66})(1 - \beta z^2)dz + +2 \int_{h}^{h+h_p} \bar{c}_{55}(1 - \beta z^2)dz$$

$$(G_{11}, G_{12}, G_{66}) = \int_{-h}^{-h} (Q_{11}, Q_{12}, Q_{66})z^3 dz$$

$$(H_{11}, H_{12}) = \int_{-h}^{-h} (Q_{11}, Q_{12})(z^4 - cz^6)dz + 2 \int_{h}^{h+h_p} (\bar{c}_{11}, \bar{c}_{12})(z^4 - cz^6)dz$$

$$H_{66} = \int_{-h}^{-h} (Q_{66})(z^4 - cz^6)dz + 2 \int_{h}^{h+h_p} (\bar{c}_{11} - \bar{c}_{12})(z^4 - cz^6)dz$$

$$(L_{11}, L_{12}) = \int_{-h}^{-h} (Q_{11}, Q_{12})cz^6 dz + 2 \int_{h}^{h+h_p} (\bar{c}_{11}, \bar{c}_{12})cz^6 dz$$

$$L_{66} = 2 \int_{-h}^{-h} (Q_{66})cz^6 dz + 2 \int_{h}^{h+h_p} (\bar{c}_{11} - \bar{c}_{12})cz^6 dz$$

$$S_{55} = \int_{-h}^{-h} (Q_{66}^b)(z^2 - \beta z^4)dz + 2 \int_{h}^{h+h_p} \bar{c}_{55}(z^2 - \beta z^4)dz \tag{A.3}$$

The constant quantities in Eq. (22), can be expressed as follow:

$$ab_1 = A_{11} + 2c\frac{F_{11}}{R_x} + c^2\frac{H_{11}}{R_x^2} + T_2 - \frac{T_8}{R_x^2} + \beta\frac{T_{8z2}}{R_x^2} - c\frac{T_{4z3}}{R_x^2}$$

$$ab_2 = A_{66} + 2c\frac{F_{66}}{R_x} + c^2\frac{H_{66}}{R_x^2}$$

$$ab_3 = \frac{1}{R_x^2}(\beta D_{55} - A_{55})$$

$$ab_4 = A_{12} + A_{66} + \frac{c}{R_y}(F_{12} + F_{66})$$

$$\quad + \frac{c}{R_x}(F_{12} + F_{66}) + \frac{c^2}{R_x R_y}(H_{12} + H_{66}) + T_2 + \frac{1}{R_x R_y}(-T_8 + \beta T_{8z2} - cT_{4z3})$$

$$ab_5 = B_{11} - cF_{11} + c\frac{G_{11}}{R_x} - c^2\frac{H_{11}}{R_x} + \frac{1}{R_x}(T_7 + T_8) - \frac{\beta}{R_x}(T_{7z2} + T_{8z2}) + \frac{c}{R_x}(T_{3z3} + T_{4z3})$$

$$ab_6 = B_{66} - c\left(F_{66} - \frac{G_{66}}{R_x}\right) - c^2\frac{H_{66}}{R_x}$$

$$ab_7 = \frac{1}{R_x}(A_{55} - \beta D_{55})$$

$$ab_8 = B_{12} + B_{66} - c(F_{12} + F_{66}) + \frac{c}{R_x}(G_{12} + G_{66})$$

$$- \frac{c^2}{R_x}(H_{12} + H_{66}) + \frac{1}{R_x}(T_7 + T_8) - \frac{\beta}{R_x}(T_{7z2} + T_{8z2}) + \frac{c}{R_x}(T_{3z3} + T_{4z3})$$

$$ab_9 = -c\left(F_{11} + \frac{c}{R_x}H_{11}\right) + \frac{1}{R_x}(T_8 - \beta T_{8z2} + cT_{4z3})$$

$$ab_{10} = -c\left(F_{12} + 2F_{66} + \frac{c}{R_x}(H_{12} + 2H_{66})\right) + \frac{1}{R_x}(T_8 - \beta T_{8z2} + cT_{4z3})$$

$$ab_{11} = \frac{1}{R_x}\left(A_{11} + A_{55} - \beta D_{55} + \frac{cF_{11}}{R_x} + \frac{A_{12}R_x}{R_y} + \frac{cF_{12}}{R_y}\right) + T_2\left(\frac{1}{R_x} + \frac{1}{R_y}\right)$$

$$ac_1 = A_{21} + A_{66} + \frac{c}{R_x}(F_{21} + F_{66}) + \frac{c}{R_y}(F_{21} + F_{66})$$

$$+ \frac{c^2}{R_x R_y}(H_{21} + H_{66}) + T_2 + \frac{1}{R_x R_y}(-T_8 + \beta T_{8z2} - cT_{4z3})$$

$$ac_2 = A_{66} + 2c\frac{F_{66}}{R_y} + c^2\frac{H_{66}}{R_y^2}$$

$$ac_3 = A_{22} + 2c\frac{F_{22}}{R_y} + c^2\frac{H_{22}}{R_y^2} + T_2 + \frac{1}{R_y^2}(-T_8 + \beta T_{8z2} - cT_{4z3})$$

$$ac_4 = \frac{1}{R_y^2}(\beta D_{44} - A_{44})$$

$$ac_5 = B_{21} + B_{66} - c(F_{21} + F_{66}) + \frac{c}{R_y}(G_{21} + G_{66})$$

$$+ \frac{1}{R_y}(T_7 + T_8) - \frac{c^2}{R_y}(H_{21} + H_{66}) + \frac{1}{R_y}(-\beta(T_{8z2} + T_{7z2}) + c(T_{4z3} + T_{3z3}))$$

$$ac_6 = B_{66} - cF_{66} + c\frac{G_{66}}{R_y} - c^2\frac{H_{66}}{R_y}$$

$$ac_7 = B_{22} - cF_{22} + c\frac{G_{22}}{R_y} - c^2\frac{H_{22}}{R_y} + \frac{1}{R_y}(T_7 + T_8)$$

$$+ \frac{1}{R_y}(-\beta(T_{8z2} + T_{7z2}) + c(T_{4z3} + T_{3z3}))$$

$$ac_8 = \frac{1}{R_y}(A_{44} - \beta D_{44})$$

$$ac_9 = -c\left(2F_{66} + F_{21} + 2\frac{c}{R_y}H_{66} + \frac{c}{R_y}H_{21}\right) + \frac{1}{R_y}(T_8 - \beta T_{8z2} + cT_{4z3})$$

$$ac_{10} = -c\left(F_{22} + \frac{c}{R_y}H_{22}\right) + \frac{1}{R_x}(T_8 - \beta T_{8z2} + cT_{4z3})$$

$$ac_{11} = \frac{1}{R_y}\left(A_{21}\frac{R_y}{R_x} + A_{22} + A_{44} - \beta D_{44} + \frac{cF_{21}}{R_x} + \frac{cF_{22}}{R_y}\right) + T_2\left(\frac{1}{R_x} + \frac{1}{R_y}\right)$$

$$ad_1 = B_{11} + \frac{c}{R_x}G_{11} - cF_{11} - \frac{c^2}{R_x}H_{11} + \frac{1}{R_x}(-T_8 + \beta T_{8z2} - cT_{4z3})A_{66}$$

$$+ 2c\frac{F_{11}}{R_x} + c^2\frac{H_{11}}{R_x^2} + T_2 - \frac{T_8}{R_x^2} + \beta\frac{T_{8z2}}{R_x^2} - c\frac{T_{4z3}}{R_x^2}$$

$$ad_2 = A_{66} + 2c\frac{F_{66}}{R_x} + c^2\frac{H_{66}}{R_x^2}$$

$$ad_3 = \frac{1}{R_x^2}(\beta D_{55} - A_{55})$$

$$ad_4 = A_{12} + A_{66} + \frac{c}{R_y}(F_{12} + F_{66}) + \frac{c}{R_x}(F_{12} + F_{66})$$
$$+ \frac{c^2}{R_x R_y}(H_{12} + H_{66}) + T_2 + \frac{1}{R_x R_y}(-T_8 + \beta T_{8z2} - cT_{4z3})$$

$$ad_5 = B_{11} - cF_{11} + c\frac{G_{11}}{R_x} - c^2\frac{H_{11}}{R_x} + \frac{1}{R_x}(T_7 + T_8) - \frac{\beta}{R_x}(T_{7z2} + T_{8z2}) + \frac{c}{R_x}(T_{3z3} + T_{4z3})$$

$$ad_6 = B_{66} - c\left(F_{66} - \frac{G_{66}}{R_x}\right) - c^2\frac{H_{66}}{R_x}$$

$$ad_7 = \frac{1}{R_x}(A_{55} - \beta D_{55})$$

$$ad_8 = B_{12} + B_{66} - c(F_{12} + F_{66}) + \frac{c}{R_x}(G_{12} + G_{66}) - \frac{c^2}{R_x}(H_{12} + H_{66})$$
$$+ \frac{1}{R_x}(T_7 + T_8) - \frac{\beta}{R_x}(T_{7z2} + T_{8z2}) + \frac{c}{R_x}(T_{3z3} + T_{4z3})$$

$$ad_9 = -c\left(F_{11} + \frac{c}{R_x}H_{11}\right) + \frac{1}{R_x}(T_8 - \beta T_{8z2} + cT_{4z3})$$

$$ad_{10} = -c\left(F_{12} + 2F_{66} + \frac{c}{R_x}(H_{12} + 2H_{66})\right) + \frac{1}{R_x}(T_8 - \beta T_{8z2} + cT_{4z3})$$

$$ad_{11} = \frac{1}{R_x}\left(A_{11} + A_{55} - \beta D_{55} + \frac{cF_{11}}{R_x} + \frac{A_{12}R_x}{R_y} + \frac{cF_{12}}{R_y}\right) + T_2\left(\frac{1}{R_x} + \frac{1}{R_y}\right)$$

$$af_1 = A_{21} + A_{66} + \frac{c}{R_x}(F_{21} + F_{66}) + \frac{c}{R_y}(F_{12} + F_{66}) + \frac{c^2}{R_x R_y}(H_{12} + H_{66})$$
$$+ T_2 + \frac{1}{R_x R_y}(-T_8 + \beta T_{8z2} - cT_{4z3})A_{66} + 2c\frac{F_{11}}{R_x} + c^2\frac{H_{11}}{R_x^2} + T_2 - \frac{T_8}{R_x^2} + \beta\frac{T_{8z2}}{R_x^2} - c\frac{T_{4z3}}{R_x^2}$$

$$af_2 = A_{66} + 2c\frac{F_{66}}{R_x} + c^2\frac{H_{66}}{R_x^2}$$

$$af_3 = \frac{1}{R_x^2}(\beta D_{55} - A_{55})$$

$$af_4 = A_{12} + A_{66} + \frac{c}{R_y}(F_{12} + F_{66}) + \frac{c}{R_x}(F_{12} + F_{66}) + \frac{c^2}{R_x R_y}(H_{12} + H_{66}) + T_2 + \frac{1}{R_x R_y}(-T_8 + \beta T_{8z2} - cT_{4z3})$$

$$af_5 = B_{11} - cF_{11} + c\frac{G_{11}}{R_x} - c^2\frac{H_{11}}{R_x} + \frac{1}{R_x}(T_7 + T_8) - \frac{\beta}{R_x}(T_{7z2} + T_{8z2}) + \frac{c}{R_x}(T_{3z3} + T_{4z3})$$

$$af_6 = B_{66} - c\left(F_{66} - \frac{G_{66}}{R_x}\right) - c^2\frac{H_{66}}{R_x}$$

$$af_7 = \frac{1}{R_x}(A_{55} - \beta D_{55})$$

$$af_8 = B_{12} + B_{66} - c(F_{12} + F_{66}) + \frac{c}{R_x}(G_{12} + G_{66}) - \frac{c^2}{R_x}(H_{12} + H_{66})$$
$$+ \frac{1}{R_x}(T_7 + T_8) - \frac{\beta}{R_x}(T_{7z2} + T_{8z2}) + \frac{c}{R_x}(T_{3z3} + T_{4z3})$$

$$af_9 = -c\left(F_{11} + \frac{c}{R_x}H_{11}\right) + \frac{1}{R_x}(T_8 - \beta T_{8z2} + cT_{4z3})$$

$$af_{10} = -c\left(F_{12} + 2F_{66} + \frac{c}{R_x}(H_{12} + 2H_{66})\right) + \frac{1}{R_x}(T_8 - \beta T_{8z2} + cT_{4z3})$$

$$af_{11} = \frac{1}{R_x}\left(A_{11} + A_{55} - \beta D_{55} + \frac{cF_{11}}{R_x} + \frac{A_{12}R_x}{R_y} + \frac{cF_{12}}{R_y}\right) + T_2\left(\frac{1}{R_x} + \frac{1}{R_y}\right)$$

$$ag_1 = \frac{1}{R_x}\left(-A_{55} + \beta D_{55} - A_{11} - \frac{c}{R_x}F_{11} - \frac{R_x}{R_y}A_{21} - \frac{c}{R_y}F_{21}\right) - T_2\left(\frac{1}{R_x} + \frac{1}{R_y}\right)$$

$$ag_2 = c\left(F_{11} + \frac{c}{R_x}H_{11}\right) + \frac{1}{R_x}(-T_8 + \beta T_{8z2} - cT_{4z3})$$

$$ag_3 = c\left(2F_{66} + 2\frac{c}{R_x}H_{66} + F_{21} + \frac{c}{R_x}H_{21}\right) + \frac{1}{R_x}(-T_8 + \beta T_{8z2} - cT_{4z3})$$

$$ag_4 = \frac{1}{R_y}\left(-A_{44} + \beta D_{44} - A_{22} - \frac{c}{R_x}F_{12} - \frac{R_y}{R_x}A_{12} - \frac{c}{R_y}F_{22}\right) - T_2\left(\frac{1}{R_x} + \frac{1}{R_y}\right)$$

$$ag_5 = c\left(F_{12} + \frac{c}{R_y}H_{12} + 2F_{66} + 2\frac{c}{R_y}H_{66}\right) + \frac{1}{R_y}(-T_8 + \beta T_{8z2} - cT_{4z3})$$

$$ag_6 = c\left(F_{22} + \frac{c}{R_y}H_{22}\right) + \frac{1}{R_y}(-T_8 + \beta T_{8z2} - cT_{4z3})$$

$$ag_7 = A_{55} - \beta D_{55} - \frac{B_{11}}{R_x} + \frac{c}{R_x}F_{11} - \frac{B_{21}}{R_y} + \frac{c}{R_y}F_{21}$$

$$ag_8 = c(G_{12} - cH_{11}) + T_7 + T_8 - \beta(T_{8z2} + T_{7z2}) + c(T_{3z3} + T_{4z3})$$

$$ag_9 = c(2G_{66} - 2cH_{66} + G_{21} - cH_{21}) + T_7 + T_8 - \beta(T_{8z2} + T_{7z2}) + c(T_{3z3} + T_{4z3})$$

$$ag_{10} = A_{44} - \beta D_{44} - \frac{B_{12}}{R_x} + \frac{c}{R_x}F_{12} - \frac{B_{22}}{R_y} + \frac{c}{R_y}F_{22}$$

$$ag_{11} = c(G_{22} - cH_{22}) + T_7 + T_8 - \beta(T_{8z2} + T_{7z2}) + c(T_{3z3} + T_{4z3})$$

$$ag_{12} = c(2G_{66} - 2cH_{66} + G_{12} - cH_{12}) + T_7 + T_8 - \beta(T_{8z2} + T_{7z2}) + c(T_{3z3} + T_{4z3})$$

$$ag_{13} = -c^2 H_{11} + T_8 - \beta T_{8z2} + cT_{4z3}$$

$$ag_{14} = -c^2 H_{22} + T_8 - \beta T_{8z2} + cT_{4z3}$$

$$ag_{15} = -c^2(4H_{66} + H_{21} + H_{12}) + 2T_8 - 2\beta T_{8z2} + 2cT_{4z3}$$

$$ag_{16} = A_{55} - \beta D_{55} + 2\frac{c}{R_x}F_{11} + \frac{c}{R_y}(F_{21} + F_{12})$$

$$ag_{17} = A_{44} - \beta D_{44} + 2\frac{c}{R_y}F_{22} + \frac{c}{R_x}(F_{21} + F_{12})$$

$$ag_{18} = -\left(\frac{A_{11}}{R_x^2} + \frac{1}{R_x R_y}(A_{12} + A_{21}) + \frac{A_{22}}{R_y^2}\right) - T_2\left(\frac{1}{R_x^2} + \frac{1}{R_x R_y}\right) - T_2\left(\frac{1}{R_y^2} + \frac{1}{R_x R_y}\right) \tag{A.4}$$

For open-circuit condition:

$$T_1 = \bar{e}_{31}\left(\int\limits_{h}^{h+h_p} \frac{\partial \varphi^t}{\partial z}\,dz + \int\limits_{-h-h_p}^{-h} \frac{\partial \varphi^b}{\partial z}\,dz\right)$$

$$T_2 = \int\limits_{h}^{h+h_p} \frac{\bar{e}_{31}^2}{\bar{\Xi}_{33}}\,dz + \int\limits_{-h-h_p}^{-h} \frac{\bar{e}_{31}^2}{\bar{\Xi}_{33}}\,dz$$

$$T_3 = \int\limits_{h}^{h+h_p} \frac{\bar{e}_{31}^2}{\bar{\Xi}_{33}}(h + h_p)\,dz - \int\limits_{-h-h_p}^{-h} \frac{\bar{e}_{31}^2}{\bar{\Xi}_{33}}(h + h_p)\,dz$$

$$T_4 = -\int\limits_{h}^{h+h_p} \frac{\bar{e}_{31}^2}{\bar{\Xi}_{33}} c(h+h_p)^3 \, dz + \int\limits_{-h-h_p}^{-h} \frac{\bar{e}_{31}^2}{\bar{\Xi}_{33}} c(h+h_p)^3 \, dz$$

$$T_5 = e_{15}\left(\int\limits_{h}^{h+h_p} \varphi^t \, dz + \int\limits_{-h-h_p}^{-h} \varphi^b \, dz\right)$$

$$T_6 = \frac{e_{15}\bar{e}_{31}}{\bar{\Xi}_{33}}\left(\int\limits_{h}^{h+h_p} (z-h)dz + \int\limits_{-h-h_p}^{-h} (z+h)dz\right)$$

$$T_7 = \frac{e_{15}\bar{e}_{31}}{\bar{\Xi}_{33}}\left(h+h_p\right)\left(\int\limits_{h}^{h+h_p} (z-h)dz - \int\limits_{-h-h_p}^{-h} (z+h)dz\right)$$

$$T_8 = c\frac{e_{15}\bar{e}_{31}}{\bar{\Xi}_{33}}\left(h+h_p\right)^3\left(-\int\limits_{h}^{h+h_p} (z-h)dz + \int\limits_{-h-h_p}^{-h} (z+h)dz\right)$$

$$T_{1z} = \bar{e}_{31}\left(\int\limits_{h}^{h+h_p} \frac{\partial\varphi^t}{\partial z}z \, dz + \int\limits_{-h-h_p}^{-h} \frac{\partial\varphi^b}{\partial z}z \, dz\right)$$

$$T_{2z} = \int\limits_{h}^{h+h_p} \frac{\bar{e}_{31}^2}{\bar{\Xi}_{33}}z \, dz + \int\limits_{-h-h_p}^{-h} \frac{\bar{e}_{31}^2}{\bar{\Xi}_{33}}z \, dz$$

$$T_{3z} = \int\limits_{h}^{h+h_p} \frac{\bar{e}_{31}^2}{\bar{\Xi}_{33}}(h+h_p)z \, dz - \int\limits_{-h-h_p}^{-h} \frac{\bar{e}_{31}^2}{\bar{\Xi}_{33}}(h+h_p)z \, dz$$

$$T_{4z} = -\int\limits_{h}^{h+h_p} \frac{\bar{e}_{31}^2}{\bar{\Xi}_{33}}cz(h+h_p)^3 \, dz + \int\limits_{-h-h_p}^{-h} \frac{\bar{e}_{31}^2}{\bar{\Xi}_{33}}cz(h+h_p)^3 \, dz$$

$$T_{1z3} = \bar{e}_{31}\left(\int\limits_{h}^{h+h_p} \frac{\partial\varphi^t}{\partial z}z^3 \, dz + \int\limits_{-h-h_p}^{-h} \frac{\partial\varphi^b}{\partial z}z^3 \, dz\right)$$

$$T_{2z3} = \int\limits_{h}^{h+h_p} \frac{\bar{e}_{31}^2}{\bar{\Xi}_{33}}z^3 \, dz + \int\limits_{-h-h_p}^{-h} \frac{\bar{e}_{31}^2}{\bar{\Xi}_{33}}z^3 \, dz$$

$$T_{3z3} = \int\limits_{h}^{h+h_p} \frac{\bar{e}_{31}^2}{\bar{\Xi}_{33}}(h+h_p)z^3 \, dz - \int\limits_{-h-h_p}^{-h} \frac{\bar{e}_{31}^2}{\bar{\Xi}_{33}}(h+h_p)z^3 \, dz$$

$$T_{4z3} = -\int\limits_{h}^{h+h_p} \frac{\bar{e}_{31}^2}{\bar{\Xi}_{33}}cz^3(h+h_p)^3 \, dz + \int\limits_{-h-h_p}^{-h} \frac{\bar{e}_{31}^2}{\bar{\Xi}_{33}}cz^3(h+h_p)^3 \, dz$$

$$T_{5z2} = e_{15}\left(\int_{h}^{h+h_p} z^2\varphi^t\,dz + \int_{-h-h_p}^{-h} z^2\varphi^b\,dz\right)$$

$$T_{6z2} = \frac{e_{15}\bar{e}_{31}}{\bar{\Xi}_{33}}\left(\int_{h}^{h+h_p} (z-h)z^2dz + \int_{-h-h_p}^{-h} (z+h)z^2dz\right)$$

$$T_{7z2} = \frac{e_{15}\bar{e}_{31}}{\bar{\Xi}_{33}}(h+h_p)\left(\int_{h}^{h+h_p} (z-h)z^2dz - \int_{-h-h_p}^{-h} (z+h)z^2dz\right)$$

$$T_{8z2} = c\frac{e_{15}\bar{e}_{31}}{\bar{\Xi}_{33}}(h+h_p)^3\left(-\int_{h}^{h+h_p} (z-h)z^2dz + \int_{-h-h_p}^{-h} (z+h)z^2dz\right) \tag{A.5}$$

and for closed-circuit condition:

$$T_1 = \bar{e}_{31}\left(\int_{h}^{h+h_p} \frac{\partial\varphi^t}{\partial z}dz + \int_{-h-h_p}^{-h} \frac{\partial\varphi^b}{\partial z}dz\right),$$

$$T_5 = e_{15}\left(\int_{h}^{h+h_p} \varphi^t dz + \int_{-h-h_p}^{-h} \varphi^b dz\right),$$

$$T_{1z} = \bar{e}_{31}\left(\int_{h}^{h+h_p} \frac{\partial\varphi^t}{\partial z}zdz + \int_{-h-h_p}^{-h} \frac{\partial\varphi^b}{\partial z}zdz\right),$$

$$T_{1z3} = \bar{e}_{31}\left(\int_{h}^{h+h_p} \frac{\partial\varphi^t}{\partial z}z^3dz + \int_{-h-h_p}^{-h} \frac{\partial\varphi^b}{\partial z}z^3dz\right),$$

$$T_{5z2} = e_{15}\left(\int_{h}^{h+h_p} z^2\varphi^t dz + \int_{-h-h_p}^{-h} z^2\varphi^b dz\right)$$

$$T_2 = T_3 = T_4 = T_6 = T_7 = T_8 = T_{2z} = T_{3z} = T_{4z} = T_{2z3} = T_{3z3} = T_{4z3} = T_{6z2} = T_{7z2} = T_{8z2} = 0, \tag{A.6}$$

Appendix B

In Eq. (26), the definitions of constant quantities are expressed as follows:

For open-circuit condition:

$$\varphi^t = 1 - \left(\frac{z - h - h_p/2}{h_p/2}\right)^2, \varphi^b = 1 - \left(\frac{-z - h - h_p/2}{h_p/2}\right)^2$$

$$S_1 = \int_{h}^{h+h_p} e_{15}(1 - \beta z^2)dz + \int_{-h-h_p}^{-h} e_{15}(1 - \beta z^2)dz$$

$$S_2 = \Xi_{11}\left(\int_{h}^{h+h_p}\varphi^t dz + \int_{-h-h_p}^{-h}\varphi^b dz\right)$$

$$S_3 = \int_{h}^{h+h_p}\bar{e}_{31}dz + \int_{-h-h_p}^{-h}\bar{e}_{31}dz$$

$$S_4 = \int_{h}^{h+h_p}\bar{e}_{31}\beta z^2 dz + \int_{-h-h_p}^{-h}\bar{e}_{31}\beta z^2 dz$$

$$S_5 = \overline{\Xi}_{33}\left(\int_{h}^{h+h_p}\frac{d^2\varphi^t}{dz^2}dz + \int_{-h-h_p}^{-h}\frac{d^2\varphi^b}{dz^2}dz\right)$$

$$S_6 = S_7 = S_8 = 0 \tag{B.1}$$

and for closed-circuit condition:

$$\varphi^t = 1 + \frac{4(z-h)}{h_p} - \left(\frac{z-h-h_p/2}{h_p/2}\right)^2$$

$$\varphi^b = 1 - \frac{4(z+h)}{h_p} - \left(\frac{-z-h-h_p/2}{h_p/2}\right)^2$$

$$S_1 = \int_{h}^{h+h_p}e_{15}\left(1-\beta z^2\right)dz + \int_{-h-h_p}^{-h}e_{15}\left(1-\beta z^2\right)dz$$

$$S_2 = \Xi_{11}\left(\int_{h}^{h+h_p}\varphi^t dz + \int_{-h-h_p}^{-h}\varphi^b dz\right)$$

$$S_3 = \int_{h}^{h+h_p}\bar{e}_{31}dz + \int_{-h-h_p}^{-h}\bar{e}_{31}dz$$

$$S_4 = \int_{h}^{h+h_p}\bar{e}_{31}\beta z^2 dz + \int_{-h-h_p}^{-h}\bar{e}_{31}\beta z^2 dz$$

$$S_5 = \overline{\Xi}_{33}\left(\int_{h}^{h+h_p}\varphi^t dz + \int_{-h-h_p}^{-h}\varphi^b dz\right)$$

$$S_6 = \frac{\Xi_{11}\bar{e}_{31}}{\overline{\Xi}_{33}}\left(\int_{h}^{h+h_p}(z-h)dz + \int_{-h-h_p}^{-h}(z+h)dz\right)$$

$$S_7 = \frac{\Xi_{11}\bar{e}_{31}}{\overline{\Xi}_{33}}\left(h+h_p\right)\left(-\int_{h}^{h+h_p}(z-h)dz + \int_{-h-h_p}^{-h}(z+h)dz\right)$$

$$S_8 = \frac{\Xi_{11}\overline{e}_{31}}{\overline{\Xi}_{33}}(h + h_p)^3 \left(\int\limits_{h}^{h+h_p} (z-h)dz - \int\limits_{-h-h_p}^{-h} (z+h)dz \right) \tag{B.2}$$

References

1. Krumhaar, H.: Investigation of the accuracy of linear piston theory when applied to cylindrical shells. AIAA J. (1963). https://doi.org/10.2514/3.1832
2. Dowell, E.H.: Panel flutter-a review of the aeroelastic stability of plates and shells. AIAA J. **8**(3), 385–399 (1970). https://doi.org/10.2514/3.5680
3. Pidaparti, R.: Flutter analysis of cantilevered curved composite panels. Compos. Struct. **25**(1–4), 89–93 (1993). https://doi.org/10.1016/0263-8223(93)90154-I
4. Cunningham, P.R., White, R.G., Aglietti, G.: The effects of various design parameters on the free vibration of doubly curved composite sandwich panels. J. Sound Vib. **230**(3), 617–648 (2000). https://doi.org/10.1006/jsvi.1999.2632
5. Kumar, L.R., Datta, P., Prabhakara, D.: Dynamic instability characteristics of laminated composite doubly curved panels subjected to partially distributed follower edge loading. Int. J. Solids Struct. **42**(8), 2243–2264 (2005). https://doi.org/10.1142/S0219455405001507
6. Zhang, W.W., Zeng, Y., Zang, C.A.: Supersonic flutter analysis based on a local piston theory. AIAA J. **47**(10), 2321–2328 (2009). https://doi.org/10.2514/1.37750
7. Oh, I.K., Kim, D.H.: Vibration characteristics and supersonic flutter of cylindrical composite panels with large thermoelastic deflections. Compos. Struct. **90**(2), 208–216 (2009). https://doi.org/10.1016/j.compstruct.2009.03.012
8. Haddadpour, H., Navazi, H., Shadmehri, F.: Nonlinear oscillations of a fluttering functionally graded plate. Compos. Struct. **79**(2), 242–250 (2007). https://doi.org/10.1016/j.compstruct.2006.01.006
9. Chorfi, S., Houmat, A.: Nonlinear free vibration of a moderately thick doubly curved shallow shell of elliptical plan-form. Int. J. Comput. Methods **6**(04), 615–632 (2009). https://doi.org/10.1142/S0219876209002030
10. Hosseini, M., Fazelzadeh, S.: Aerothermoelastic post-critical and vibration analysis of temperature-dependent functionally graded panels. J. Therm. Stresses **33**(12), 1188–1212 (2010). https://doi.org/10.1080/01495739.2010.510754
11. Kiani, Y., Shakeri, M., Eslami, M.: Thermoelastic free vibration and dynamic behaviour of an FGM doubly curved panel via the analytical hybrid Laplace-Fourier transformation. Acta Mech. **223**(6), 1199–1218 (2012). https://doi.org/10.1007/s00707-012-0629-9
12. Li, F.M., Song, Z.G.: Aeroelastic flutter analysis for 2D Kirchhoff and Mindlin panels with different boundary conditions in supersonic airflow. Acta Mech. **225**(12), 3339–3351 (2014). https://doi.org/10.1007/s00707-014-1141-1
13. Shen, H.S., Chen, X., Guo, L., Wu, L., Huang, X.L.: Nonlinear vibration of FGM doubly curved panels resting on elastic foundations in thermal environments. Aerosp. Sci. Technol. **47**, 434–446 (2015). https://doi.org/10.1016/j.ast.2015.10.011
14. Wattanasakulpong, N., Chaikittiratana, A.: An analytical investigation on free vibration of FGM doubly curved shallow shells with stiffeners under thermal environment. Aerosp. Sci. Technol. **40**, 181–190 (2015). https://doi.org/10.1016/j.ast.2013.12.002
15. Ganji, H.F., Dowell, E.H.: Panel flutter prediction in two-dimensional flow with enhanced piston theory. J. Fluids Struct. **63**, 97–102 (2016). https://doi.org/10.1016/j.jfluidstructs.2016.03.003
16. Grover, N., Singh, B., Maiti, D.: An inverse trigonometric shear deformation theory for supersonic flutter characteristics of multilayered composite plates. Aerosp. Sci. Technol. **52**, 41–51 (2016). https://doi.org/10.1016/j.ast.2016.02.017
17. MalekzadehFard, K., Shokrollahi, S.: Higher order flutter analysis of doubly curved sandwich panels with variable thickness under aerothermoelastic loading. Struct. Eng. Mech. **60**(1), 1–19 (2016). https://doi.org/10.12989/sem.2016.60.1.001
18. Sankar, A., Natarajan, S., Ben Zine, T., Ganapathi, M.: Investigation of supersonic flutter of thick doubly curved sandwich panels with CNT reinforced face sheets using higher-order structural theory. Compos. Struct. **127**, 340–355 (2015). https://doi.org/10.1016/j.compstruct.2015.02.047
19. Song, M., Kitipornchai, S., Yang, J.: Free and forced vibrations of functionally graded polymer composite plates reinforced with graphene nanoplatelets. Compos. Struct. **159**, 579–588 (2017). https://doi.org/10.1016/j.compstruct.2016.09.070
20. Zare Jouneghani, F., Dimitri, R., Bacciocchi, M., Tornabene, F.: Free vibration analysis of functionally graded porous doubly-curved shells based on the first-order shear deformation theory. Appl. Sci. **7**(12), 1252 (2017). https://doi.org/10.3390/app7121252
21. Rezaei, A.S., Saidi, A.R., Abrishamdari, M., PourMohammadi, M.H.: Natural frequencies of functionally graded plates with porosities via a simple four variable plate theory: an analytical approach. Thin-Walled Struct. **120**, 366–377 (2017). https://doi.org/10.1016/j.tws.2017.08.003
22. Pouresmaeeli, S., Fazelzadeh, S.A., Ghavanloo, E., Marzocca, P.: Uncertainty propagation in vibrational characteristics of functionally graded carbon nanotube-reinforced composite shell panels. Int. J. Mech. Sci. **149**, 549–558 (2018). https://doi.org/10.1016/j.ijmecsci.2017.05.049
23. Lei, Z.X., Zhang, L.W., Liew, K.M., Yu, J.L.: Dynamic stability analysis of carbon nanotube-reinforced functionally graded cylindrical panels using the element-free KP-Ritz method. Compos. Struct. **113**, 328–338 (2014). https://doi.org/10.1016/j.compstruct.2014.03.035
24. Shahverdi, H., Khalafi, V., Noori, S.: Aerothermoelastic analysis of functionally graded plates using generalized differential quadrature method. Lat. Am. J. Solids Struct. **13**(4), 796–818 (2016). https://doi.org/10.1590/1679-78252072
25. Navazi, H., Haddadpour, H.: Aero-thermoelastic stability of functionally graded plates. Compos. Struct. **80**(4), 580–587 (2007). https://doi.org/10.1016/j.compstruct.2006.07.014
26. Kiani, Y.: Free vibration of FG-CNT reinforced composite spherical shell panels using Gram–Schmidt shape functions. Compos. Struct. **159**, 368–381 (2017). https://doi.org/10.1016/j.compstruct.2016.09.079

27. Mehar, K., Panda, S.K., Patle, B.K.: Thermoelastic vibration and flexural behaviour of FG-CNT reinforced composite curved panel. Int. J. Appl. Mech. **9**(04), 1750046 (2017). https://doi.org/10.1142/S1758825117500466

28. Zhou, J., Xu, M., Yang, Z.: Aeroelastic stability analysis of curved composite panels with embedded Macro Fiber Composite actuators. Compos. Struct. **208**, 725–734 (2019). https://doi.org/10.1016/j.compstruct.2018.10.035

29. Lin, H., Cao, D., Xu, Y.: Vibration, buckling and aeroelastic analyses of functionally graded multilayer graphene-nanoplatelets-reinforced composite plates embedded in piezoelectric layers. Int. J. Appl. Mech. **10**(03), 1850023 (2018). https://doi.org/10.1142/S1758825118500230

30. Saidi, A.R., Bahaadini, R., Majidi-Mozafari, K.: On vibration and stability analysis of porous plates reinforced by graphene platelets under aerodynamical loading. Compos. B Eng. **164**, 778–799 (2019). https://doi.org/10.1016/j.compositesb.2019.01.074

31. Bahaadini, R., Saidi, A.R., Majidi-Mozafari, K.: Aeroelastic flutter analysis of thick porous plates in supersonic flow. Int. J. Appl. Mech. **11**(10), 1950096 (2019). https://doi.org/10.1142/S1758825119500960

32. Muc, A., Flis, J., Augustyn, M.: Optimal design of plated/shell structures under flutter constraints—a literature review. Materials **12**(24), 4215 (2019). https://doi.org/10.3390/ma12244215

33. Arani, A.G., Kiani, F., Afshari, H.: Aeroelastic analysis of laminated FG-CNTRC cylindrical panels under yawed supersonic flow. Int. J. Appl. Mech. **11**(06), 1950052 (2019). https://doi.org/10.1142/S1758825119500522

34. Aditya, S., Haboussi, M., Shubhendu, S., Ganapathi, M., Polit, O.: Supersonic flutter study of porous 2D curved panels reinforced with graphene platelets using an accurate shear deformable finite element procedure. Compos. Struct. **241**, 112058 (2020). https://doi.org/10.1016/j.compstruct.(2020).112058

35. Bahaadini, R., Saidi, A.R., Hosseini, M.: Dynamic stability of fluid-conveying thin-walled rotating pipes reinforced with functionally graded carbon nanotubes. Acta Mech. **229**, 5013–5029 (2018). https://doi.org/10.1007/s00707-018-2286-0

36. Majidi, M.H., Azadi, M., Fahham, H.: Effect of CNT reinforcements on the flutter boundaries of cantilever trapezoidal plates under yawed supersonic fluid flow. Mech. Based Des. Struct. Mach. (2020). https://doi.org/10.1080/15397734.2020.1723107

37. Esmaeili, H., Kiani, Y., Beni, Y.T.: Vibration characteristics of composite doubly curved shells reinforced with graphene platelets with arbitrary edge supports. Acta Mech. (2022). https://doi.org/10.1007/s00707-021-03140-z

38. An, X.M., Sun, W.: Study of aeroelastic response of cylindrical composite panels in A high-speed flow. Int. J. Modern Phys. B **34**(14n16), 2040116 (2020). https://doi.org/10.1142/S0217979220401165

39. Ye, L., Ye, Z., Ye, K., Wu, J.: Aeroelastic stability and nonlinear flutter analysis of viscoelastic heated panel in shock-dominated flows. Aerosp. Sci. Technol. **117**, 106909 (2021). https://doi.org/10.1016/j.ast.2021.106909

40. Rahmanian, M., Javadi, M.: Supersonic aeroelasticity and dynamic instability of functionally graded porous cylindrical shells using a unified solution formulation. Int. J. Struct. Stab. Dyn. **20**(12), 2050132 (2020). https://doi.org/10.1142/S0219455420501321

41. Adamian, A., Hosseini Safari, K., Sheikholeslami, M., Habibi, M., Alforjan, M.S.H., Chen, G.: Critical temperature and frequency characteristics of GPLs-reinforced composite doubly curved panel. Appl. Sci. **10**(9), 3251 (2020). https://doi.org/10.3390/app10093251

42. Zhou, X., Wang, Y., Zhang, W.: Vibration and flutter characteristics of GPL-reinforced functionally graded porous cylindrical panels subjected to supersonic flow. Acta Astronaut. **183**, 89–100 (2021). https://doi.org/10.1016/j.actaastro.2021.03.003

43. AminYazdi, A.: Flutter of geometrical imperfect functionally graded carbon nanotubes doubly curved shells. Thin-Walled Struct. **164**, 107798 (2021). https://doi.org/10.1016/j.tws.2021.107798

44. Subramani, M., Subramani, M., Ramamoorthy, M., Arumugam, A.B., Selvaraj, R.: Free and forced vibration characteristics of CNT reinforced composite spherical sandwich shell panels with MR elastomer core. Int. J. Struct. Stab. Dyn. **21**(10), 2150136 (2021). https://doi.org/10.1142/S0219455421501364

45. Majidi Mozafari, K., Bahaadini, R., Saidi, A.R.: Aeroelastic flutter analysis of functionally graded spinning cylindrical shells reinforced with graphene nanoplatelets in supersonic flow. Mater. Res. Express **8**(11), 115012 (2021). https://doi.org/10.1088/2053-1591/ac2ce4

46. Abdollahi, M., Saidi, A.R., Bahaadini, R.: Aeroelastic analysis of symmetric and non-symmetric trapezoidal honeycomb sandwich plates with FG porous face sheets. Aerosp. Sci. Technol. **119**, 107211 (2021). https://doi.org/10.1016/j.ast.2021.107211

47. Merdaci, S., Adda, H.M., Hakima, B., Dimitri, R., Tornabene, F.: Higher-order free vibration analysis of porous functionally graded plates. J. Compos. Sci. **5**(11), 305 (2021). https://doi.org/10.3390/jcs5110305

48. Houshangi, A., Jafari, A.A., Haghighi, S.E., Nezami, M.: Supersonic flutter characteristics of truncated sandwich conical shells with MR core. Thin-Walled Struct. **173**, 108888 (2022). https://doi.org/10.1016/j.tws.2022.108888

49. Chen, J., Han, R., Liu, D., Zhang, W.: Active flutter suppression and aeroelastic response of functionally graded multilayer graphene nanoplatelet reinforced plates with piezoelectric patch. Appl. Sci. **12**(3), 1244 (2022). https://doi.org/10.3390/app12031244

50. Arani, A.G., Eskandari, M., Haghparast, E.: The supersonic flutter behavior of sandwich plates with a magnetorheological elastomer core and GNP-reinforced face sheets. Int. J. Appl. Mech. (2022). https://doi.org/10.1142/S1758825122500156

51. Khorshidi, K., Karimi, M., Amabili, M.: Aeroelastic analysis of rectangular plates coupled to sloshing fluid. Acta Mech. **231**, 3183–3198 (2020). https://doi.org/10.1007/s00707-020-02696-6

52. Crawley, E.F., De Luis, J.: Use of piezoelectric actuators as elements of intelligent structures. AIAA J. **25**(10), 1373–1385 (1987). https://doi.org/10.2514/3.9792

53. Zhou, R.C., Lai, Z., Xue, D.Y., Huang, J.K., Mei, C.: Suppression of nonlinear panel flutter with piezoelectric actuators using finite element method. AIAA J. **33**(6), 1098–1105 (1995). https://doi.org/10.2514/3.12530

54. Song, Z.G., Li, F.M.: Active aeroelastic flutter analysis and vibration control of supersonic composite laminated plate. Compos. Struct. **94**(2), 702–713 (2012). https://doi.org/10.1016/j.compstruct.2011.09.005

55. Li, F.M.: Active aeroelastic flutter suppression of a supersonic plate with piezoelectric material. Int. J. Eng. Sci. **51**, 190–203 (2012). https://doi.org/10.1016/j.ijengsci.2011.10.003

56. Tsushima, N., Su, W.: Flutter suppression for highly flexible wings using passive and active piezoelectric effects. Aerosp. Sci. Technol. **65**, 78–89 (2017). https://doi.org/10.1016/j.ast.2017.02.013

57. Li, F.M., Chen, Z.B., Cao, D.Q.: Improving the aeroelastic flutter characteristics of supersonic beams using piezoelectric material. J. Intell. Mater. Syst. Struct. **22**(7), 615–629 (2011). https://doi.org/10.1177/1045389X11403820
58. Xue, Y., Li, J., Li, F., Song, Z.: Flutter and thermal buckling properties and active control of functionally graded piezoelectric material plate in supersonic airflow. Acta Mech. Solida Sin. **33**(5), 692–706 (2020). https://doi.org/10.1007/s10338-020-00159-y
59. Wang, Q., Quek, S.T., Sun, C.T., Liu, X.: Analysis of piezoelectric coupled circular plate. Smart Mater. Struct. **10**(2), 229 (2001). https://doi.org/10.1088/0964-1726/10/2/308
60. Farsangi, M.A., Saidi, A.: Levy type solution for free vibration analysis of functionally graded rectangular plates with piezoelectric layers. Smart Mater. Struct. **21**(9), 094017 (2012). https://doi.org/10.1088/0964-1726/21/9/094017
61. Almeida, A., Donadon, M.V., De Faria, A.R., Almeida, S.F.M.: The effect of piezoelectrically induced stress stiffening on the aeroelastic stability of curved composite panels. Compos. Struct. **94**(12), 3601–3611 (2012). https://doi.org/10.1016/j.compstruct.2012.06.008
62. Zhang, L., Song, Z., Liew, K.: Computation of aerothermoelastic properties and active flutter control of CNT reinforced functionally graded composite panels in supersonic airflow. Comput. Methods Appl. Mech. Eng. **300**, 427–441 (2016). https://doi.org/10.1016/j.cma.2015.11.029
63. Tian, W., Zhao, T., Yang, Z.: Nonlinear electro-thermo-mechanical dynamic behaviours of a supersonic functionally graded piezoelectric plate with general boundary conditions. Compos. Struct. **261**, 113326 (2021). https://doi.org/10.1016/j.compstruct.2020.113326
64. Tham, V., Tran, H., Tu, T.: Vibration characteristics of piezoelectric functionally graded carbon nanotube-reinforced composite doubly-curved shells. Appl. Math. Mech. **42**(6), 819–840 (2021). https://doi.org/10.1007/s10483-021-2730-7
65. Reddy, J.N.: Mechanics of Laminated Composite Plates and Shells: Theory and Analysis. CRC Press, Boca Raton (2004)
66. Ebrahimi, F., Jafari, A.: A higher-order thermomechanical vibration analysis of temperature-dependent FGM beams with porosities. J. Eng. (2016). https://doi.org/10.1155/2016/9561504
67. Dowell, E.H.: Aeroelasticity of Plates and Shells, vol. 1. Springer Science & Business Media, Berlin (1974)
68. Wattanasakulpong, N., Ungbhakorn, V.: Linear and nonlinear vibration analysis of elastically restrained ends FGM beams with porosities. Aerosp. Sci. Technol. **32**(1), 111–120 (2014). https://doi.org/10.1016/j.ast.2013.12.002
69. Farsangi, M.A., Saidi, A.R., Batra, R.C.: Analytical solution for free vibrations of moderately thick hybrid piezoelectric laminated plates. J. Sound Vib. **332**(22), 5981–5998 (2013). https://doi.org/10.1016/j.jsv.2013.05.010
70. Murakami, H.: Laminated composite plate theory with improved in-plane responses. J. Appl. Mech. **53**(1), 661–666 (1986)
71. Sciuva, D.M.: An improved shear-deformation theory for moderately thick multilayered anisotropic shells and plates. J. Appl. Mech. **54**(1), 589–596 (1987)
72. Matsunaga, H.: Free vibration and stability of functionally graded shallow shells according to a 2D higher-order deformation theory. Compos. Struct. **84**(2), 132–146 (2008). https://doi.org/10.1016/j.compstruct.2007.07.006
73. Akbari, H., Azadi, M., Fahham, H.: Flutter prediction of cylindrical sandwich panels with saturated porous core under supersonic yawed flow. Proc. Inst. Mech. Eng. C J. Mech. Eng. Sci. **235**(16), 2968–2984 (2021). https://doi.org/10.1177/0954406220960786
74. Prakash, T., Ganapathi, M.: Supersonic flutter characteristics of functionally graded flat panels including thermal effects. Compos. Struct. **72**(1), 10–18 (2006). https://doi.org/10.1016/j.compstruct.2004.10.007
75. Fung, Y.: On two-dimensional panel flutter. J. Aerosp. Sci. **25**(3), 145–160 (1958). https://doi.org/10.2514/8.7557